

63-3-3

ASD-TR-62-962

403 049

403049

**THEORY OF THE COMPRESSIBLE LAMINAR
BOUNDARY LAYER UNDER ARBITRARY
PRESSURE AND TEMPERATURE GRADIENTS**

CATALOGED BY ASTIA
AS AD NO. _____

TECHNICAL DOCUMENTARY REPORT NO. ASD-TR-62-962

MARCH 1963

FLIGHT DYNAMICS LABORATORY
AERONAUTICAL SYSTEMS DIVISION
AIR FORCE SYSTEMS COMMAND
WRIGHT-PATTERSON AIR FORCE BASE, OHIO

Project No. 1366; Task No. 136606

ASTIA
RECEIVED
MAY 7 1963

(Prepared under Contract AF 33(616)-7827
by The Ohio State University Research Foundation, Columbus, Ohio
Author: Theodore C. Nark)

NOTICES

When Government drawings, specifications, or other data are used for any purpose other than in connection with a definitely related Government procurement operation, the United States Government thereby incurs no responsibility nor any obligation whatsoever; and the fact that the Government may have formulated, furnished, or in any way supplied the said drawings, specifications, or other data, is not to be regarded by implication or otherwise as in any manner licensing the holder or any other person or corporation, or conveying any rights or permission to manufacture, use, or sell any patented invention that may in any way be related thereto.

Qualified requesters may obtain copies of this report from the Armed Services Technical Information Agency, (ASTIA), Arlington Hall Station, Arlington 12, Virginia.

This report has been released to the Office of Technical Services, U.S. Department of Commerce, Washington 25, D.C., in stock quantities for sale to the general public.

Copies of this report should not be returned to the Aeronautical Systems Division unless return is required by security considerations, contractual obligations, or notice on a specific document.

B

FOREWORD

This report was prepared by the Aerodynamic Laboratory of the Ohio State University, Columbus, Ohio on Air Force Contract AF 33(616)-7827 under Task 136606, "Hypersonic Boundary Layer Properties," on Project No. 1366, "Aerodynamic and Flight Mechanics." This Task and Project are a part of Air Force System Command's Applied Research Program, 750A, "Mechanics of Flight." The work was administered under the direction of the Flight Dynamics Laboratory, Aeronautical Systems Division. Captain H. Grubbs and Mr. M. L. Buck were project engineers for the Laboratory.

ABSTRACT

An analysis is presented which can predict the compressible laminar boundary layer characteristics on a blunt flat plate with prescribed surface temperature and pressure gradients. The analysis uses a Von Karman integral method to solve the compressible momentum and energy equations. Problems usually encountered with very high pressure gradients are avoided by employing a new velocity profile which remains undistorted. A first-order analysis of the effect of entropy gradients in the inviscid flow on the boundary layer parameters is also given.

PUBLICATION REVIEW

This report has been reviewed and is approved.

FOR THE COMMANDER

Philip P. Antonatos
PHILIP P. ANTONATOS
Chief, Flight Branch
Flight Dynamics Laboratory

TABLE OF CONTENTS

	PAGE
Nomenclature	vii
SECTION	
I INTRODUCTION	1
II ANALYTIC METHOD FOR PREDICTING THE PRESSURE DISTRIBUTION ABOUT BLUNT BODIES AT ZERO ANGLE-OF-ATTACK	3
III SELECTION OF THE METHOD FOR PREDICTING THE SHOCK-WAVE SHAPE	5
IV THEORETICAL ANALYSIS	6
V SOLUTION FOR THE ADIABATIC WALL CASE	16
VI STAGNATION POINT ANALYSIS FOR TWO-DIMENSIONAL BLUNT BODIES	17
VII DISCUSSION	21
VIII CONCLUSIONS	26
APPENDICES	
I Derivation of the Energy Integral Equation for Use at the Stagnation Point	27
II Approximate Relationship Between $\frac{T}{T_s}$ and $\frac{h}{h_s}$	29
III Derivation of $\left(\frac{dF_1}{dX}\right)_0$	30
IV Derivation of $\left[\frac{d\psi}{dX}\right]_0$	36
V Method of Numerical Solution	38
VI Derivation of the Equations for Use with Strong Favorable Streamwise Pressure Gradients	41
VII Method for Predicting Adiabatic Wall Temperatures	44
Bibliography	46

LIST OF ILLUSTRATIONS

FIGURE		PAGE
1	Pressure Distribution Over a Cylindrical Body at $M_1 = 6.86$	50
2	Pressure Distribution Over a Cylindrical Body at $M_1 = 12.28$	51
3	Effect of Angle of Attack on the Pressure Distribution Over a Cylindrical Leading Edge	52
4	Hypersonic Blast Wave Analogy	53
5	Effect of Reynolds Number on Surface Pressure at $M = 12.2$	54
6	Correlation of the Pressure Distribution Over Cylindrical Leading Edges	55
7	Effect of M_1 on Correlation of Surface Pressures	56
8	Pressure Gradient Over a Cylindrical Body at $M_1 = 12.28$	57
9	Pressure Gradient Over a Blunt Flat Plate at $M_1 = 12.2$	58
10	Shock Wave Profiles at $M_1 = 12.28$	59
11	Coordinate Systems and Body Geometry	60
12	Behaviour of the Recovery Factor at the Wall with P_{r_w}	61
13	Behaviour of the Local Recovery Factor	62
14	Stagnation Point Heat Transfer Comparison	63
15	Stagnation Point Heat Transfer Correlation	64
16	Approximation to the Behaviour of a Real Gas	65

TABLE

1	Summary of Stagnation Point Heat Transfer Calculations	49
---	--	----

NOMENCLATURE

- A, B** Constants in the Approximate Temperature-Enthalpy Relationship
- a_i** Coefficients in the Entropy Profile of Equation (7-10)
- a** (i) Speed of Sound
(ii) Profile Parameter - Defined in Equation (7-1)
- b_i** $b_{11} = \int_1 \frac{h_{aw} - h_w}{h_w}$
- C** Constant in Chapman-Rubens Viscosity Relationship
- C_n** Nose Drag Coefficient
- d** Leading Edge Diameter
- E** Energy Per Unit Mass
- F(x)** Defined in Equation (6-10)
- G₁(K)** Defined in Equation (III-2)
- G₂(K)** Defined in Equation (III-2)
- G₃(K₁)** Defined in Equation (III-2)
- G₄(K)** Defined in Equation (III-4)
- g₁** Defined in Equation (III-22)
- g₂** Defined in Equation (6-9)
- h** Enthalpy per Unit Mass
- K** $K = \Delta \left[\frac{\theta}{\Delta} \right]^2$
- K₁(η)** $K_1(\eta) = 4\eta^3 - 3\eta^4$
- K₂(η)** $K_2(\eta) = \eta - 3\eta^3 + \eta^4$
- K₃(η)** $K_3(\eta) = \eta^2 - 2\eta^3 + \eta^4$
- k** Coefficient of Thermal Conductivity
- M** Mach Number
- m** Mass Flow Per Unit Time

N	Co-ordinate Normal to the Streamline	
n	Transformed Co-ordinate	
P	Pressure	
P_n	$P_n = \frac{P}{\rho}$	
Pr	Prandtl Number	
q	Heat Transfer Parameter	
r	(i) Recovery Factor (ii) Leading Edge Radius	
Re	$Re = \frac{\rho U \cdot d}{\mu}$	
S	Entropy/Mass	
S	Entropy/Area	
T	Absolute Temperature	
T_n	$T_n = \frac{T_s}{T_w}$	
u	Velocity	
u'	$u' = \frac{du}{dx}$	
x', z	Shock Wave Co-ordinates	
x', z'	Non-dimensional Shock Wave Co-ordinates	$x'_w = \frac{x'}{d}, z'_w = \frac{z'}{d}$
x, y	Co-ordinate System Defined in Figure 11	
x_w	$x_w = \frac{x}{d}$	
α_i	Coefficients in the Velocity Profile	
α	Angle-of-attack	
β	Defined in Equation (IV-30)	
γ	Ratio of Specific Heats	
δ	Boundary Layer Thickness	
δ*	Displacement Thickness	
Δ	Pressure Gradient Parameter in the Velocity Profile	
ψ₀, ψ_n	Defined in Figure 11	

θ	Momentum Thickness
θ_w	Shock Wave Angle Defined in Figure 11
θ_e	Energy Thickness
ϕ	Radial Angle - Defined in Figure 11
κ	Normal Shock Wave Density Ratio
η	Non-dimensional Transformed Co-ordinate $\eta = \frac{y}{\delta}$
τ	Local Shear Stress
ρ	Density
f_i	Coefficients in the Equilibrium Enthalpy Profile
f	Vorticity
f_i^*	Coefficients in the Non-equilibrium Enthalpy Profile
Δ	Transformed Boundary Layer Thickness
μ	Coefficient of Viscosity
λ	$\lambda = \frac{y - \delta}{y_e - \delta}$

Subscripts

aw	Conditions at an Adiabatic Wall
e	Conditions Pertaining to an Equilibrium Boundary Layer
$M.P.$	Conditions at the Match Point
s	Conditions on Downstream Side of the Shock Wave
\dagger	Stagnation Conditions
w	(i) Shock Wave Conditions (ii) Wall Conditions
o	Stagnation Point Conditions
1	Conditions Directly Upstream of a Normal Shock Wave
2	Conditions Directly Downstream of a Normal Shock Wave
δ	Conditions at the Outer Edge of the Boundary Layer
n	Pertaining to Conditions at Station X_n
S_n	Conditions Downstream of the Shock Wave at Station X_n

I. INTRODUCTION

The use of blunt bodies to alleviate the severe heating problems associated with atmospheric re-entry vehicles has generated a considerable amount of interest in determining the boundary layer characteristics about blunt bodies in hypersonic flow. During a large portion of the re-entry trajectory the boundary layer will be entirely laminar and there is some hope for an analytic solution, at least in the regime where the Prandtl boundary layer approximations are valid. This report presents an attempt at solving the compressible laminar boundary layer equations for a blunt flat plate at a zero angle-of-attack. The only attendant restrictions are these:

1. Prandtl's boundary layer assumptions are valid.
2. The viscosity is linearly dependent on temperature.
3. The pressure distribution on the body is available.
4. The wall temperature distribution is defined.
5. The shock-wave shape can be predicted.

Consistent with the above restrictions, the analysis will be capable of predicting:

1. Boundary layer profiles for temperature, enthalpy and velocity.
2. Local skin friction coefficient.
3. Local heat transfer coefficient.
4. Total-pressure gradient along the outer edge of the boundary layer.
5. Variation of the boundary layer thickness along the plate.
6. Variation of the momentum, energy, and displacement thicknesses along the plate.

The literature contains many special or restricted solutions to the laminar compressible boundary layer equations. These solutions usually contain various combinations of the following restrictions:

1. Zero pressure gradient.
2. Zero surface temperature gradient.
3. Prandtl number equal to unity.
4. Adiabatic wall condition.
5. Incompressible flow.
6. Very specific pressure gradients.

Manuscript released by author 19 October 1962 for publication as an ASD Technical Documentary Report.

7. Linear viscosity-temperature relationship.

8. Boundary layer and shock wave coincide.

One of the earliest solutions of the compressible laminar boundary layer equations was given by Chapman and Rubesin (1).* They were the first to use the linear viscosity-temperature relationship

$$\frac{\mu}{\mu_s} = c \frac{T}{T_s} \quad (1-1)$$

to separate the energy and momentum equations. Unfortunately their analysis does not account for the effects of pressure gradient.

Basically the present analysis applies the Von Karman integral method to obtain the solution of the compressible laminar boundary layer equations for any arbitrary pressure and temperature distributions. A good reference to previous works utilizing the integral approach for a solution to the laminar boundary layer equations as well as a critical analysis of their short-coming is contained in the introductory section of a paper by Beckwith (2). The analysis of Beckwith has the disadvantage that it cannot be applied to a problem with a surface temperature gradient. The introductory section of NACA TN-3157 by Libby and Morduchow (3) gives another good review of the papers using the integral method to solve the compressible laminar boundary layer equations. The analysis of NACA TN-3157 is only valid for an axial pressure gradient with a uniform wall temperature or a zero pressure gradient with an arbitrary wall temperature distribution.

The analysis of this paper, in addition to being valid for a flat plate with a wide range of pressure and temperature distributions, can be extended to encompass the solution of three-dimensional axially-symmetric blunt bodies at zero angle-of-attack, as well as blunt (or sharp) flat plates at moderate angles-of-attack.

The only severe restriction on the solution is the linear dependence of the viscosity on temperature. The analysis by Chapman and Rubesin (1) to define the error involved by using the linear relationship instead of the more accurate Sutherland law concluded that "regardless of Mach number, free-stream temperature, or average surface temperature, the approximation

$$\frac{\mu}{\mu_\infty} = c \frac{T}{T_\infty}$$

can be made to yield nearly correct values for the viscosity in the important region near the surface." They then show that the approximate viscosity law does not introduce an error of more than 5 or 6 per cent over the range of free stream temperatures from 72°R to 648°R and a Mach number over the plate of 5. The maximum error in the boundary layer parameters obtained by the analysis of this paper attributed to using the linear viscosity-temperature relationship instead of the Sutherland equation could be expected then to be around 5 or 6 per cent since in hypersonic flow the Mach number over the plate never gets much higher than 5 and there is reason to believe that the error is not a strong function of temperature.

*Numbers in parentheses denote references listed in the bibliography.

To start the analysis the shock-wave shape, the surface temperature distribution, and the pressure distribution existing on the body must be known. Part of the problem of solving for the boundary layer characteristics is to define both the pressure distribution and shock-wave shape consistent with the body shape and free-stream Mach number. One method of obtaining the pressure distribution about a blunt flat plate at very high free-stream Mach numbers is taken up in Section II. A method of predicting the shock-wave shape is discussed in Section III. The methods selected for defining the shock-wave shape and pressure distribution will be pointed towards applications in hypersonic flow where at present the greatest interest seems to lie. This does not in any way detract from the usefulness of the analysis at any steady-state supersonic flow condition.

II. ANALYTIC METHOD FOR PREDICTING THE PRESSURE DISTRIBUTION ABOUT BLUNT BODIES AT ZERO ANGLE-OF-ATTACK

The pressure distribution over the body must be known before the boundary layer equations can be solved by the Von Karman integral method. In the past an integral analysis itself, to which another constraint has been added, has been used to predict the pressure distribution (4). This added constraint was to assume that the shock wave lies right on the boundary layer. This constraint has been criticized by some (5) as not being representative of the physical conditions, consequently it is not used in this analysis. Instead, a method of predicting the pressure distribution will be used which has been found to be very successful (6). The method basically consists of predicting the pressure distribution on the cylindrical leading edge using the Prandtl-Meyer plus Newtonian analysis as proposed by Lees and Kubota (6) and using the hypersonic blast-wave analogy to define the pressure distribution on the afterbody.

In the nose region it has been found experimentally that the Newtonian corpuscular theory as modified by Lees adequately predicts the pressure distribution on a cylindrical leading edge up to a point about 35° from the shoulder. Lees and Kubota (6) in attempting to predict the pressure distribution to the shoulder tried matching a Prandtl-Meyer expansion to the Newtonian solution. The point at which the two methods were joined was defined to be that point at which the pressures and $dP/d\phi$ predicted by both analyses are the same. The above conditions together with the condition that the total pressure was assumed constant around to the shoulder allowed one to calculate the angle ϕ_{MP} and Mach number M_{MP} at the match point as a function of the free-stream Mach number. A plot of the variation in ϕ_{MP} and M_{MP} with free-stream Mach number is found in reference (7). Fortunately the pressure distribution generated by such an analysis has been shown experimentally to predict the inviscid pressures about a blunt body around to the shoulder. It will not account for any induced pressure effects.

A comparison of the non-dimensional pressure distribution, P/P_∞ , as predicted by the Prandtl-Meyer plus modified Newtonian analysis, is made in Figures 1 and 2. The experimental data at $M_1 = 6.86$ (Figure 1) were obtained from reference (8) and the experimental data at $M_1 = 12.28$ (Figure 2) from reference (9). From Figures 1 and 2 it can be seen that the modified Newtonian plus Prandtl-Meyer analysis can be considered as a satisfactory approximation of the pressure distribution around the cylindrical leading edge. It might be noted that in both cases, the blunt body was a complete cylinder and the effect of an afterbody is not well known. In reference (9), a cylindrically blunted flat plate was tested at moderate angles-of-attack;

Figure 3 presents a portion of the data showing that the forebody pressures are not influenced by these angles-of-attack. Somewhat conflicting results were obtained in reference (10), a series of tests on a flat plate of slightly different configuration than the blunted slab of reference (9). As shown in Figure 3, it appears that the distributions are affected by the afterbody at angles-of-attack. Whether these differences can be attributed to experimental scatter, Reynolds number, or to model configuration, or whether the forebody pressures are indeed influenced by afterbody shape will have to be resolved by further experiment.

It must be kept in mind, however, that this representation neglects the effects of Reynolds number as well as surface temperature distribution. Extreme care must be taken to insure that a method of predicting pressures around blunt leading edges is not used in situations where it is not applicable, i.e., flow conditions where severe merging of the boundary layer and shock wave caused an induced pressure to alter the inviscid (Prandtl-Meyer plus Newtonian) solution appreciably. Along this line the analysis of reference (11) will prove invaluable.

The pressures on the afterbody can be determined from the hypersonic flow-blast wave analogy. It has been demonstrated (12) that the equations of motion of the hypersonic small disturbance theory (13) are analogous to the equations of motion for unsteady shock wave flow (14, 15, 16, 17, 18). The analysis of Lees and Kubota (6) indicates that in particular the analogy is a valid one for the case of hypersonic flow over a flat plate with a cylindrical leading edge. The analogy is an important one when it is recognized that the blast-wave equations (equations of motion for unsteady shock waves) have been solved many times (14, 15, 16, 17, 18) and as a consequence of the analogy these solutions represent a solution to the equation of motion of the hypersonic small disturbance theory. Lukasiewicz (19) develops equations for defining the surface pressures and shock-wave shape applicable to a blunt flat plate from the solution of the blast-wave equations of Sakurai (14, 15). The paper by Lukasiewicz is also an excellent survey paper pertaining to the hypersonic flow-blast wave analogy.

Sakurai presents two solutions to the blast-wave equations. In both solutions the basic property of the analysis is the power series representation for ρ , ρ' , and u in terms of the inverse shock wave Mach number $[a_1/\mu_w]$. For very strong explosions the speed of sound, a_1 , will be very much smaller than the wave speed, μ_w . The first solution keeps the linear terms in $[a_1/\mu_w]$ (14) and the second solution the terms up to $[a_1/\mu_w]^2$ (15). In addition to the approximate solutions of Sakurai (14, 15) the blast-wave equations have an exact solution which was determined by Sedov (16). The exact solution of Sedov agrees with Sakurai's first-order solution, being 5.2 per cent larger at all values of x/d , but does not agree nearly as well with Sakurai's second-order solution. A comparison of the solutions of Sedov (16) and Sakurai (14, 15) with experimental data is made in Figure 4. It is evident from Figure 4 that the exact solution of Sedov does not represent the data as well as Sakurai's second-order solution. This is not too alarming, however, since in developing the hypersonic small disturbance theory the linearization process could easily account for the discrepancy between the experimental data and the exact solution of the linearized equations of motion. It might also be noted that the over-all agreement is the poorest in the vicinity of the nose region. This is what might be expected because it is in the nose region that the assumption that the body slopes be small, which effectively means that the velocity disturbances are small, is invalid. All available correlation of theory with experimental data indicates that the blast-wave theory is valid approximately for $X_x \geq 2$ or 3.

The equation which best defines the pressure distribution over a blunt flat plate, as obtained from Sakurai's second-order solution, is

$$\frac{P}{P_1} = .121 M_1^2 \left[\frac{C_{0w}}{X_w} \right]^{\frac{2}{3}} + 0.56 \quad (2-1)$$

The term C_{0w} in equation (2-1) is analogous to the initial energy of the explosion in the blast-wave equations and its full significance is explained in reference (6). The above theory as applied to hypersonic flow has the disadvantage that it does not account for any effects of heat transfer or surface temperature distribution. Fortunately it seems from an analysis of experimental data that this is not too severe a limitation, at least not of the order of magnitude of the next problem. The initial hypersonic analysis assumed inviscid flow and at low free-stream Reynolds numbers it might be expected that an interaction between the boundary layer and shock wave could alter the inviscid pressure distribution over the plate. This Reynolds number effect is illustrated in Figure 5, where experimental pressure data from reference (9) have been plotted. It can be seen that the experimental data at a Reynolds number of 11,900 do not agree with the second-order blast-wave theory as well as the data taken at the higher Reynolds numbers.

The pressure distribution in the vicinity of the shoulder, where both methods discussed are not applicable, is obtained by joining the data from the Prandtl-Meyer expansion with that of the blast-wave theory with a reasonably smooth curve. It is noteworthy to mention that if the data for the pressure over the plate from both theoretical analyses are expressed in the form P/P_1 vs X_w , they will generate one curve for $M_1 \geq 8$. This would lead one to the conclusion that the predominant parameter defining the pressure on the blunt flat plate is the impact pressure downstream of the normal shock and not the free-stream Mach number. This conclusion is borne out for the leading edge region by the experimental data as shown in Figure 6. The pressures on the afterbody do not correlate in quite the same manner as shown in Figure 7 where the data of reference (9) are plotted for three different Mach numbers all with the same P_2 and T_{r_2} . The correlation is not as Mach-number independent as the theory would indicate.

In addition to the pressure distribution on the body the pressure gradient term dp/dx must also be known in order to obtain a solution. In analyzing the gradient term from the Prandtl-Meyer plus Newtonian analysis it was noticed that, although the pressure gradients at the match point are equal, the curvature or second derivative of the pressure with respect to x is not continuous. In the non-dimensional plot of the pressure gradient dP/dX_w versus X_w (Figure 8) this appears as a discontinuity in the slope. Figures 8 and 9 present a comparison between experimentally and theoretically determined pressure gradients. From a comparison of the data presented in Figures 8 and 9 it can be concluded that for the purposes of a boundary layer analysis the theoretically determined pressure gradients are an acceptable approximation to the experimental data.

III. SELECTION OF THE METHOD FOR PREDICTING THE SHOCK-WAVE SHAPE

As previously mentioned, in order to arrive at a numerical solution for the boundary layer characteristics the shape of the shock wave in the vicinity of the

stagnation point must be known. The stagnation region is of primary interest because all the mass flow in the boundary layer will have passed through the strong portion of the shock wave, that portion of the shock wave which is in the vicinity of the forward stagnation point. Three methods were examined in detail before one was selected to predict the shock-wave shape around the test body (20, 21, 22). A plot of the shock wave in the vicinity of the stagnation point as predicted by the methods of references 20, 21, and 22 is shown in Figure 10. Fortunately the three methods, although differing in complexity, predict basically the same shock-wave shape near the stagnation point. Consequently, since there was no appreciable difference among the three methods, the one easiest to adapt to our particular situation was selected. This was the method of reference (20). The shock-wave shape is represented by

$$z^2 = 2x_w' \left[1 + \frac{2}{3(K-1)} \right], \quad (3-1)$$

where K is the normal shock density ratio.

References 20, 21, and 22 are by no means the only papers available for predicting shock-wave shapes. These references were selected because each satisfied the high Mach number restriction. If an analysis is to be carried out at a lower Mach number, the particular method chosen to predict the shape at Mach 12 cannot be applied since it is an hypersonic approximation. But there are other methods for predicting shock-wave shape (23) which would work equally well with this analysis.

IV. THEORETICAL ANALYSIS

This analysis presents a method of solving the compressible boundary layer equations for a blunt flat plate at zero angle-of-attack. The main purpose of the analysis is to determine the boundary layer characteristics on a blunt flat plate, without referring to any experimental data if possible. The only restrictions imposed on the analysis are the following:

1. The pressure distribution on the body is available.
2. The shock-wave shape can be predicted.
3. The wall temperature distribution is defined.
4. The viscosity is linearly dependent on temperature.
5. Prandtl's boundary layer assumptions are valid.

The restrictions (1) and (2) were anticipated in sections II and III where analytical methods for obtaining the shock-wave shape and the pressure distribution on the body were discussed. Restriction (3) can be relaxed if the adiabatic wall condition is analyzed and in effect the adiabatic wall temperatures can be defined for a flat plate with a pressure gradient. Restriction (4) was discussed in Section I and it was shown that the error to be expected is less than 6 per cent. Inherent in (5) is the fact that $\frac{\partial p}{\partial y} = 0$. This expression for $\frac{\partial p}{\partial y}$ fails in the region

where the boundary layer thickness is large compared to the local radius of curvature of the body. The cylindrical leading edge of the blunt flat plate under analysis is highly curved, and consequently the analysis to follow will be valid only for conditions where $\delta \ll r$.

Consider the flow model shown in Figure 11. All the mass in the boundary layer at the station X_n has passed through the shock wave between the stagnation streamline ψ_0 and the streamline ψ_n . Since the streamline is being followed from the point where it crosses the shock wave to the point where it enters the boundary layer, the mass in the streamtube crossing the shock wave between ψ_0 and ψ_n must be equal to the mass in the boundary layer at X_n . If the mass crossing the shock wave between ψ_0 and ψ_n is

$$m_1 = \rho_1 u_1 z_1 \quad (4-1)$$

and the mass in the boundary layer at X_n is

$$m_n = \int_0^{\delta} \rho u dy \quad (4-2)$$

then by equating the two expressions for mass flow the following equation is obtained,

$$z_1 = \frac{\rho_s u_s}{\rho_1 u_1} \int_0^{\delta} \frac{\rho u}{\rho_s u_s} dy \quad (4-3)$$

where the subscript " δ " refers to conditions at the outer edge of the boundary layer. The term $\rho_s u_s$ can be taken under the integral sign because it is not a 'y'-dependent term.

In order to make the analysis effectively one of constant density, the Dorodnitsyn transformation is used. It can be written,

$$\rho/\rho_s dy = dn \quad (4-4)$$

or if $n = \frac{y}{\Delta}$, where Δ is the boundary layer thickness in the transformed co-ordinate system, it can be written as

$$\rho/\rho_s dy = \Delta dn \quad (4-5)$$

Transforming the co-ordinates in equation (4-3) in accordance with equation (4-5) the following equation results:

$$z_1 = \frac{\rho_s u_s}{\rho_1 u_1} \Delta \int_0^1 \frac{u}{u_s} dn \quad (4-6)$$

Now following the method of Von Karman the velocity ratio $\frac{u}{u_s}$ is assumed to be expressible as

$$\frac{u}{u_\delta} = \sum_{i=0}^4 \alpha_i \eta^i \quad (4-7)$$

In effect the unknown boundary layer profile has been traded for five unknown constants in a fourth-order polynomial in η . To solve for the five coefficients five boundary conditions on the profile are needed. It has been shown (3) that it is advantageous to distribute the boundary conditions equally between the wall and the outer edge. For this analysis the boundary conditions will be chosen as

1. $y = \delta \ (\eta = 1) , \ \frac{u}{u_\delta} = 1$
2. $y = \delta \ (\eta = 1) , \ \frac{du}{dy} = 0$
3. $y = \delta \ (\eta = 1) , \ \frac{d^2u}{dy^2} = 0$
4. $y = 0 \ (\eta = 0) , \ u = 0$ (4-8)

The fifth boundary condition is obtained by evaluating the momentum equation at the wall. If this is done, one obtains the following expression:

$$5. \quad y = 0 \ (\eta = 0) , \ \left(\frac{dP}{dx} \right)_w = \left[\frac{\partial}{\partial y} \left(\mu \frac{\partial u}{\partial y} \right) \right]_w \quad (4-9)$$

The first three boundary conditions of equation (4-8) state that the velocity at the outer edge of the boundary layer is u_δ and that there is no change in the first or second derivative of u with respect to y at the outer edge of the boundary layer. When there are entropy gradients in the inviscid flow field, the second and third boundary condition will have to be modified. This will be further discussed in Section VII. The fourth boundary condition states that the velocity adjacent to the wall is identically zero.

As is usually done, the boundary conditions of equation (4-8) are used to define coefficients $\alpha_0, \alpha_1, \alpha_3$ and α_4 as a function of α_2 and then equation (4-9) is considered the defining equation for α_2 . If this is done, the following polynomial for u/u_δ is obtained,

$$\frac{u}{u_\delta} = 2\eta - 2\eta^3 + \eta^4 + \frac{\Delta}{6} [\eta - 3\eta^2 + 3\eta^3 - \eta^4] \quad (4-10)$$

where $-2\alpha_2 = \Delta$. Introducing the expression for $\frac{u}{u_\delta}$ of equation (4-10) in equation (4-9) and evaluating the resulting integral, the following equation is obtained,

$$z_* = \frac{\rho_s u_\delta}{\rho_i u_i} \frac{\Delta}{d} \left[\frac{7}{10} + \frac{\Delta}{120} \right] \quad (4-11)$$

In evaluating the integral $\int_0^y \frac{\mu}{u_s} dn$ it has been assumed that $\Lambda = f(\eta)$. This will now be shown to be the case by evaluating the fifth boundary condition, equation (4-9). It is at this point in the analysis that the Chapman-Rubesin viscosity-temperature relationship is used.

The most accurate viscosity relationship with which the term $(\frac{\partial \mu}{\partial T})_w$ could be determined is that of Sutherland, at least in the range of temperatures likely to be encountered on a blunt body in hypersonic flow; however, it is difficult to incorporate into the integral analysis. The problems presented by the Sutherland law can be circumvented by using the Chapman-Rubesin viscosity-temperature relationship. It is expected that their relationship will introduce errors no larger than 5 or 6 per cent.

Using the result that $dp/dy = 0$ (obtained from an order of magnitude analysis of the y-momentum equation), the Dorodnitsyn transformation, equation (4-5), can be written

$$\frac{\partial}{\partial y} = \frac{1}{\Delta} \frac{T_s}{T} \frac{\partial}{\partial \eta} \quad (4-12)$$

Utilizing the Chapman-Rubesin viscosity model,

$$\frac{\mu}{\mu_s} = C \frac{T}{T_s} \quad (4-13)$$

in conjunction with the Dorodnitsyn transformation, equation (4-12), and the polynomial expression for the velocity, equation (4-10), the momentum equation at the wall, equation (4-9), can be used to define Λ in the following manner,

$$\Lambda = \left(-\frac{dp}{dx}\right)_w \frac{\Delta^2}{u_s \mu_w} \frac{1}{T_w^2} \quad (4-14)$$

It is evident from the above equation that Λ , the velocity boundary layer shape parameter, is only a function of x and not y and consequently the integration performed to obtain equation (4-11) is valid. In many applications equation (4-14) will be used as an expression for Δ^2 as a function of x in the following form,

$$\Delta^2 = \frac{\Lambda u_s \mu_w T_w^2}{(-dp/dx)} \quad (4-15)$$

The compressible momentum integral equation can be written, following the analysis of Schlichting (24), as

$$\frac{d\theta}{dx} = -\frac{\theta}{u_s} \frac{du}{dx} \left[2 + \frac{\delta^*}{\theta} - M_\infty^2 \right] + \frac{\mu_w}{\rho_s u_s^2} \left(\frac{\partial u}{\partial y}\right)_w, \quad (4-16)$$

where θ is the momentum thickness and δ^* the displacement thickness. Evaluating $(\partial u / \partial y)_w$ from equation (4-10) with the help of the Dorodnitsyn transformation,

equation (4-12), using the compressible Bernoulli equation,

$$\frac{du}{dx} = \frac{1}{\rho_s u_s} \left(-\frac{dp}{dx} \right), \quad (4-17)$$

to eliminate the velocity gradient and then multiplying both sides of equation (4-16) by the momentum thickness, θ , results in the following equation:

$$\frac{d\theta^2}{dx} = \frac{2\mu_w T_w^2}{\rho_w u_s} \frac{\theta}{\Delta} \left\{ \left(\frac{\Delta}{\delta} + 2 \right) \frac{1}{T_w} - \Delta \frac{\theta}{\Delta} (2 + \delta^* - M_\delta^*) \right\}. \quad (4-18)$$

Equation (4-18) is the compressible momentum integral equation in the form it will be used in the numerical calculations.

The terms δ^*/θ and θ/Δ which appear in equation (4-18) have yet to be evaluated. Then momentum thickness, θ , can be defined as

$$\theta = \int_0^\delta \frac{\rho u}{\rho_s u_s} \left[1 - \frac{u}{u_s} \right] dy. \quad (4-19)$$

Applying the Dorodnitsyn transformation in the form of equation (4-5) and then evaluating the resulting integral, one obtains the following expression for the momentum thickness:

$$\frac{\theta}{\Delta} = \frac{1}{315} \left[37 - \frac{\Delta}{3} - \frac{5\Delta^2}{144} \right], \quad (4-20)$$

where it is noted that $\frac{\theta}{\Delta}$ has the same form as in incompressible flow. If the term δ^*/θ is written as $\frac{\delta^*}{\Delta} / \frac{\theta}{\Delta}$, then it is evident that an expression for the non-dimensional displacement thickness $\frac{\delta^*}{\Delta}$ is still needed.

The evaluation of $\frac{\delta^*}{\Delta}$ is not as straightforward as was the evaluation of $\frac{\theta}{\Delta}$. The displacement thickness in the η -plane can be written as

$$\frac{\delta^*}{\Delta} = \int_0^1 \left[\frac{T}{T_s} - \frac{u}{u_s} \right] d\eta, \quad (4-21)$$

where again the fact that $\frac{d\theta}{dy} = 0$ has been used. The integral $\int_0^1 \frac{u}{u_s} d\eta$ has already been shown to equal $\left[\frac{7}{10} + \frac{\Delta}{120} \right]$ and with this the displacement thickness may be written,

$$\frac{\delta^*}{\Delta} = \int_0^1 \frac{T}{T_s} d\eta - \frac{7}{10} - \frac{\Delta}{120}. \quad (4-22)$$

This is the expression that will be used to evaluate $\frac{\delta^*}{\Delta}$ for use in the numerical calculations. More will be said later concerning the evaluation of the integral

$$\int_0^1 \frac{T}{T_s} d\eta.$$

The term θ^2 which appears in the momentum integral equation is evaluated from the expressions for θ/Δ (equation (4-20)) and Δ^* (equation (4-15)) in the following manner,

$$\theta^2 = \left[\frac{\theta}{\Delta} \right]^2 \cdot \Delta^2 \quad (4-23)$$

Again consider the sketch shown in Figure 11. Since the total enthalpy of the flow is unaffected by passing through the shock wave, the streamline ψ_n enters the boundary layer at X_n with free-stream total enthalpy. In contrast to the conservation of mass analysis, where the free-stream mass and the mass at X_n were equated, the energy in the free stream between ψ_0 and ψ_n cannot be equated to the energy in the boundary layer at X_n because there has been a net heat transfer to the wall. It can be accounted for by summing up the energy lost to the wall between $X=0$ and $X=X_n$. The energy balance can then be written

$$\rho_s u_s h_{t,s} z_1 = \int_0^\delta \rho u h_t dy + \int_0^{X_n} -q_w dx, \quad (4-24)$$

where $\rho_s u_s h_{t,s} z_1$ is the free-stream energy in the unit streamtube bounded by ψ_0 and ψ_n , $\int_0^\delta \rho u h_t dy$ is the energy contained in the boundary layer at station X_n and $\int_0^{X_n} -q_w dx$ is the heat lost to the wall (or added to the boundary layer depending on the wall temperatures). If both sides of equation (4-24) are divided by $\rho_s u_s h_{t,s}$, and then the Dorodnitsyn transformation (equation (4-4)) is applied, the resulting equation is

$$\int_0^1 \frac{y}{u_s} \left[1 - \frac{h_t}{h_{t,s}} \right] d\eta = \frac{1}{\rho_s u_s h_{t,s} \Delta} \int_0^X -q_w dx, \quad (4-25)$$

where equation (4-6) has been used to simplify the above expression.

If the energy thickness is defined as

$$\theta_H \equiv \int_0^\delta \frac{\rho u}{\rho_s u_s} \left[1 - \frac{h_t}{h_{t,s}} \right] dy, \quad (4-26)$$

then $\frac{\theta_H}{\Delta}$ can be obtained, by applying the transformation from y to η (equation (4-4)), as

$$\frac{\theta_H}{\Delta} = \int_0^1 \frac{y}{u_s} \left[1 - \frac{h_t}{h_{t,s}} \right] d\eta. \quad (4-27)$$

This definition of $\frac{\theta_H}{\Delta}$ allows the energy equation (equation (4-25)) to be written as

$$\frac{\theta_H}{\Delta} = \frac{1}{\rho_s u_s h_{t,s} \Delta} \int_0^{X_n} -q_w dx \quad (4-28)$$

The parameter $\frac{\theta_+}{\delta}$ will be evaluated after a suitable polynomial expression for h/h_+ has been defined. As it stands, equation (4-28) is basically the energy integral equation and will be used to define the heat transfer characteristics of the body.

For purposes of evaluating the parameter $\frac{\theta_+}{\delta}$ the total enthalpy in the boundary layer can be assumed to have the form

$$h_t = h_{t,e} - [1 - g(\eta)] [h_{aw} - h_w], \quad (4-29)$$

where

$$h_{t,e} = h_{aw} + k(\eta) [h_{t,+} - h_{aw}]. \quad (4-30)$$

Equation (4-30) represents the total enthalpy distribution for the situation where the wall is at the adiabatic temperature. The expression for the total enthalpy profile through a boundary layer with heat transfer is represented as perturbation of the adiabatic wall condition in equation (4-29).

The function $k(\eta)$ is assumed to have the form

$$k(\eta) = \sum_{i=0}^4 f_i \eta^i. \quad (4-31)$$

The following boundary conditions define the coefficients f_i in equation (4-31):

1. $y = \delta \quad (\eta = 1) \quad , \quad h_{t,e} = h_{t,+} .$
2. $y = \delta \quad (\eta = 1) \quad , \quad \frac{dh_{t,e}}{d\eta} = 0 .$
3. $y = 0 \quad (\eta = 0) \quad , \quad h_{t,e} = h_{aw} .$
4. $y = 0 \quad (\eta = 0) \quad , \quad \frac{dh_{t,e}}{d\eta} = 0 . \quad (4-32)$

Physically the first boundary condition expresses the fact that at the outer edge of the boundary layer the total enthalpy of the equilibrium boundary layer is equal to the free-stream total enthalpy. The secondary boundary condition is tied into the first in that it says all of the fluid beyond the outer edge of the boundary layer has a constant total enthalpy equal to the free-stream total enthalpy. The third boundary condition states that equilibrium total enthalpy of the fluid adjacent to the wall is obtained by considering the fluid at the wall temperature and pressure. The fourth boundary condition arises from the fact that for zero heat transfer to the wall the temperature gradient at the wall $\frac{\partial T}{\partial y} = 0$, and consequently $\frac{dh_{t,e}}{dy} = 0$.

Applying the boundary conditions of equation (4-32) to the expression for the equilibrium total enthalpy distribution the following equation is obtained for h_{te}

$$h_{te}(\eta) = h_{aw} + [h_{+} - h_{aw}] [K_1(\eta) + \int_2 K_2(\eta)]. \quad (4-33)$$

The term \int_2 arises because there were only four boundary conditions specified to determine five coefficients, and just as was done with the velocity profile four of the coefficients were determined as a function of the fifth.

Again a fourth-order polynomial of the form

$$g(\eta) = \sum_{i=0}^4 \mathfrak{F}_i \eta^i \quad (4-34)$$

is used to evaluate the distribution of total enthalpy through the boundary layer. The boundary conditions which define the coefficients in equation (4-34) are:

1. $y = \delta \quad (\eta = 1) \quad , \quad h_{+} = h_{+} .$
 2. $y = \delta \quad (\eta = 1) \quad , \quad \frac{dh_{+}}{dy} = 0 .$
 3. $y = 0 \quad (\eta = 0) \quad h_{+} = h_{w} .$
- (4-35)

The first boundary condition stems from the fact that at the outer edge of the boundary layer the total enthalpy of the boundary layer reaches the free-stream value. The second condition indicates that the local rate of change of the total enthalpy is zero at the outer edge of the boundary layer. The third condition states that at the wall the total enthalpy of the fluid may be obtained from the surface pressure and wall temperature. This time there are only three boundary conditions with which to solve for five unknown coefficients. Consequently any three of the coefficients can be determined as a function of the other two. Carrying out the indicated calculation the expression for $h_{+}(\eta)$ becomes,

$$h_{+}(\eta) = K_1(\eta) [h_{+} - h_{w}] + K_2(\eta) [h_{aw} - h_{w}] \mathfrak{F}_1 + K_3(\eta) [\int_2 (h_{+} - h_{aw}) + \int_2 (h_{aw} - h_{w})], \quad (4-36)$$

where equation (4-33) has been substituted for $h_{te}(\eta)$. There are three coefficients in equation (4-36) which still must be determined, \mathfrak{F}_1 , \mathfrak{F}_2 , and \mathfrak{F}_3 .

The expressions for \mathfrak{F}_1 and \mathfrak{F}_2 can be obtained by considering the energy equation evaluated at the wall,

$$\left[\frac{\partial}{\partial y} \left(k \frac{\partial T}{\partial y} \right) \right]_w + \mu_w \left(\frac{\partial u}{\partial y} \right)_w^2 = 0 \quad (4-37)$$

Expanding equation (4-37), using the Chapman-Rubesin expression to represent the thermal conductivity, k , and applying the Dorodnitsyn transformation (equation (4-12)), the expression that will be used to determine f_2 and f_2' becomes

$$\left[\frac{\partial^2 T}{\partial \eta^2} \right]_w + \frac{Pr_{ew}}{C_{p_w}} \left[\frac{\partial u}{\partial \eta} \right]_w^2 = 0 \quad (4-38)$$

At this point in the analysis the above equation will be used to determine f_2' . Using the basic definition for the specific heat at constant pressure, $C_p = \frac{\partial h}{\partial T}$, to convert from a temperature derivative to an enthalpy derivative and then using the equilibrium enthalpy distribution (equation (4-33)) to evaluate the enthalpy derivative at the wall the expression for f_2' becomes

$$f_2' = (1 - Pr_{ew}) \frac{h_{+1} - h_5}{h_{+1} - h_{aw}} \left[\frac{\Delta}{6} + 2 \right]^2, \quad (4-39)$$

where $(\partial u / \partial \eta)_w$ was evaluated using the velocity distribution function (equation (4-10)). Applying the same procedure but using the enthalpy distribution of equation (4-36) to evaluate the enthalpy derivative the expression for f_2 becomes

$$f_2 = \left(\frac{\partial C_p}{\partial T} \right)_w f_1' \frac{h_{aw} - h_w}{2 C_{p_w}^2} \quad (4-40)$$

If

$$b_{11} = f_1 \frac{h_{aw} - h_w}{h_{+1}} \quad (4-41)$$

then the total enthalpy distribution through the boundary layer may be expressed as a function of the coefficient b_{11} and η in the following manner,

$$h_T(\eta) = h_w + K_1(\eta) (h_{+1} - h_w) + K_2(\eta) b_{11} h_{+1} + K_3(\eta) \left\{ (1 - Pr_{ew}) (h_{+1} - h_5) \left(\frac{\Delta}{6} + 2 \right)^2 + \left(\frac{\partial C_p}{\partial T} \right)_w \frac{h_{+1} b_{11}^2}{2 C_{p_w}^2} \right\}. \quad (4-42)$$

The functions $K_1(\eta)$, $K_2(\eta)$ and $K_3(\eta)$ are the only terms dependent on the variable η in the expression for the total enthalpy distribution. If equation (4-42) is divided by h_{+1} , and the resulting expression substituted for h_T/h_{+1} ,

equation (4-27), then the expression for $\frac{\theta_w}{\Delta}$ can be developed to the point where it can be written as

$$\frac{\theta_w}{\Delta} = \frac{h_{t_1} - h_w}{h_{t_1}} \left[\frac{137}{420} + \frac{\Delta}{144} \right] - b_{11} \left[\frac{263}{2520} + \frac{5\Delta}{3024} \right] - \frac{b_{11}^2}{2} \left(\frac{\partial c_p}{\partial T} \right)_w \frac{h_{t_1}}{c_{p_w}^2} - \frac{h_{t_1} - h_\delta}{h_{t_1}} \left[(1 - P_{R_w}) \left(\frac{\Delta}{6} + 2 \right)^2 \left(\frac{\theta}{315} + \frac{\Delta}{3024} \right) \right]. \quad (4-43)$$

The expression for the shock-wave shape, which was developed in Section III, will now be used to obtain some relationships which are necessary to complete a numerical solution. The equation defining the shock wave, equation (3-1), can be differentiated once to obtain the slope,

$$\frac{dz_w}{dx_w} = \tan \theta_w = \frac{3\kappa - 1}{3(\kappa - 1)z_w}, \quad (4-44)$$

where θ_w is defined in Figure 11. Equation (4-44) can be considered as a relationship between θ_w and z_w , with another relationship between θ_w and P_{R_s} existing in the oblique shock tables (25), or effectively there exists a definite dependence of P_{R_s} on z_w . Consequently, given a z_w , the total pressure drop across a bow wave experienced by a streamline passing through the shock wave at z_w can be determined. Now at any station X_n that is being analyzed the static pressure at the edge of the boundary layer is known. From the total and static pressure at the edge of the boundary layer and the free-stream total enthalpy, the static temperature at the edge of the boundary layer can be determined. As yet the total pressure has not been defined as a unique function of X_n (i.e., the relationship between z_w and X_n is not yet known). Consequently, at each station X_n for which the analysis is carried out, a curve of z_w vs T_δ must be drawn. Such a curve is effectively one equation in the two unknowns z_w and T_δ . With a knowledge of T_δ and P_δ reference 26 can be used to define h_δ such that u_δ can be obtained from

$$u_\delta = \left[2(h_{t_1} - h_\delta) \right]^{\frac{1}{2}}. \quad (4-45)$$

Equation (4-45), in conjunction with the curve of z_w vs T_δ is sufficient to permit a curve of z_w vs u_δ to be drawn at each station. Continuing in basically the same manner, and employing reference 26, it is possible to plot a curve of γ_δ vs z_w and M_δ vs z_w at each station. Such curves come in very handy when a numerical solution is being obtained by use of a desk calculator.

The local heat transfer q_w at any point can be determined from the following equation,

$$-q_w = k_w \left(\frac{dT}{dy} \right)_w. \quad (4-46)$$

Applying the Dorodnitsyn transformation and converting the temperature derivative to an enthalpy derivative, the heat transfer at the wall can be written

$$-q_w = \frac{\mu_w T_*}{Pr_w} \frac{1}{\Delta} h_{+1} b_n, \quad (4-47)$$

where the enthalpy derivative has been evaluated using the enthalpy distribution of equation (4-36).

The local shear stress at any point can be determined by considering the equation

$$\tau_w = \mu_w \left(\frac{\partial u}{\partial y} \right)_w. \quad (4-48)$$

Evaluating $(\partial u / \partial y)_w$ from the polynomial expression for the velocity profile (equation (4-10)) the local shear stress can be written

$$\tau_w = \frac{\mu_w T_*}{\Delta} u_s \left[\frac{\Delta}{6} + 2 \right]. \quad (4-49)$$

V. SOLUTION FOR THE ADIABATIC WALL CASE

In Section IV an expression for θ_w / Δ as a function of Δ was developed (equation (4-43)) for a condition of heat transfer to the wall. This term could also be developed starting with the total enthalpy distribution applicable for zero heat transfer (equation (4-33)). The integration of equation (4-27) leads to the following expression for application to the case of zero heat transfer:

$$\frac{\theta_w}{\Delta} = \frac{h_{+1} - h_{aw}}{h_{+1}} \left\{ \left(\frac{137}{420} + \frac{\Delta}{144} \right) - \int_2 \left(\frac{8}{316} + \frac{\Delta}{3024} \right) \right\}. \quad (5-1)$$

By examining the energy integral equation it can be shown that $\frac{\theta_w}{\Delta} = 0$ for the adiabatic wall solution. For the condition of zero heat transfer the term involving the integral of $-q_w$ in equation (4-28) is identically zero and hence $\frac{\theta_w}{\Delta}$ must also be zero. This being the case, equation (5-1) becomes the second expression for \int_2 , the first being equation (4-39). If \int_2 is eliminated from both equations the following equation results,

$$1 - r_w = \frac{\frac{8}{316} + \frac{\Delta}{3024}}{\frac{137}{420} + \frac{\Delta}{144}} \left(\frac{\Delta}{6} + 2 \right)^2 (1 - Pr_w), \quad (5-2)$$

where r_w , the recovery factor at the wall, has been defined as

$$r_w = \frac{h_{aw} - h_s}{h_{+1} - h_s}. \quad (5-3)$$

On a blunt body, such as the one being analyzed, the pressure gradient parameter Λ is always positive. This is shown in equation (4-14) where Λ is expressed as a function of, among other terms, $(-\frac{dP}{dx})_w$. The term $(-\frac{dP}{dx})_w$ is positive everywhere on the plate (see Figures 8 and 9) as are the other terms in the expression for Λ , consequently Λ itself must always be positive. A plot of the recovery factor at the wall is shown in Figure 12 for Prandtl numbers of .57, .72, and .77.

The local recovery factor r varies through the boundary layer as a function of η where

$$r = \frac{h_{te}(\eta) - h_s}{h_{t1} - h_s} \quad (5-4)$$

Substituting the enthalpy distribution for zero heat transfer into equation (5-4), the following expression for the local recovery factor is obtained

$$r = r_w + (1 - r_w) K_1(\eta) + (1 - P_{r_w}) \left(\frac{\Lambda}{6} + 2\right)^2 K_2(\eta) \quad (5-5)$$

where equation (5-1) has been used to replace \int_2 in equation (4-33). A plot of the local recovery factor for $P_{r_w} = .72$ is shown in Figure 13 for Λ of -6, 0, and 6.

Equation (5-2) can be considered an expression between T_w , T_s , and Λ . Employing it in the system of equations derived in Section IV, it becomes possible to define the adiabatic wall temperatures consistent with a given pressure distribution. Consequently, the integral analysis can be used to predict the surface temperature distribution for flow over an adiabatic flat plate with a finite pressure gradient. One such method is outlined in Appendix VII.

VI. STAGNATION POINT ANALYSIS FOR TWO-DIMENSIONAL BLUNT BODIES

In order to start the step-by-step solution of the system of equations derived in section IV it is necessary to evaluate the parameters $d\theta^2/dx$ and θ^2 at the stagnation point. The momentum integral equation for a compressible fluid can be expressed as

$$\frac{d\theta^2}{dx} = \frac{2\mu_w T_s^3}{\rho_w u_s} \frac{\theta}{\Delta} \left\{ \left(\frac{\Lambda}{6} + 2\right)^2 \frac{1}{T_w} - \frac{\theta}{\Delta} \Lambda \left[2 + \frac{\delta''}{\theta} - M_s^2 \right] \right\} \quad (4-1d)$$

The energy integral equation as developed in Appendix I (a different form, but a more classical expression than that of section IV) can be written

$$\frac{d\theta_H^2}{dx} = \frac{2\mu_w T_s^3}{\rho_w u_s} \frac{\theta_H}{\Delta} \left\{ \frac{b_{11}}{P_{r_w} T_s} + \Lambda \frac{\theta_H}{\Delta} (M_s^2 - 1) \right\} \quad (6-1)$$

Equations (4-18) and (6-1), as they stand, are not applicable at the stagnation point because u_s , which appears in the denominator of both equations, is zero at a stagnation point. Consequently the derivatives take the indeterminate form

$$\frac{d\theta^2}{dx} = \frac{\theta(\Delta, b_{11}, X)}{0},$$

$$\frac{d\theta_w^2}{dx} = \frac{\theta_w(\Delta, b_{11}, X)}{0}. \quad (5-2)$$

The only possible way for equation (6-2) to have a finite value at $X = 0$ would be for $d\theta^2/dx$ and $d\theta_w^2/dx$ to be of the form $0/0$. The values Δ and b_{11} which force the numerator of equations (4-18) and (6-1) to go to zero simultaneously will be the stagnation point solution for Δ and b_{11} . With the values of Δ and b_{11} so determined, values for the derivatives in equation (6-2) can be determined in the limit (if they exist) by applying L'Hospital's rule.

Two equations in the two unknowns, Δ_0 and $b_{11,0}$, can be obtained by setting the bracketed terms in equations (4-18) and (6-1) equal to zero. The resulting equations are

$$\frac{\Delta_0}{6} + 2 = T_* \Delta_0 \left[2 \frac{\theta}{\Delta} + \frac{\delta^*}{\Delta} \right]_0, \quad (5-3)$$

$$b_{11,0} = Re_w T_* \Delta_0 \left(\frac{\theta_w}{\Delta} \right)_0, \quad (6-4)$$

where the M_s^2 terms have been dropped because they are zero at the stagnation point.

In order to solve equations (5-3) and (6-4) for $b_{11,0}$ and Δ_0 , an analytic expression must be developed for δ^*/Δ . An expression has to be obtained for T/T_s in terms of η in order to evaluate the integral in equation (4-22). This choice cannot be an arbitrary one since an expression for T/T_s has already been defined. That is, we actually define the boundary layer temperature profile when the total enthalpy (equation (4-35)) and velocity distributions (equation (4-10)) are defined. At the stagnation point where $h_+ = h$, since u_s is everywhere zero, the temperature distribution is only a function of the total enthalpy distribution. The problem now arises of finding an expression for T/T_s as a function of h/h_+ , so that the integral of equation (4-22) can be analytically integrated. Now in the most general case, enthalpy is a complicated function of both pressure and temperature and an explicit relationship $T = T(h)$ is not generally available. However, it is always possible to arrive at some good approximate expression for $T = T(h)$ when certain restrictions are placed on the range of temperature and pressure variation.

An approximate expression of this type has been developed in Appendix II. The resulting equation has the following form

$$\frac{T}{T_s} = .92 \frac{h}{h_s} + .08, \quad (5-5)$$

and has the following restrictions:

1. $360^\circ \leq T_c \leq 2700^\circ R.$
2. $360^\circ \leq T \leq 2700^\circ R.$
3. $.001 \leq \frac{P_c}{P_{21}} \leq 10$. (6-6)

Applying equation (6-5) to the integral in equation (4-22) and then substituting for the enthalpy ratio the enthalpy profile function (equation (4-35)), there results the following expression for δ^*/Δ , valid only at a stagnation point,

$$\left(\frac{\delta^*}{\Delta}\right)_0 = -0.3 - \frac{\Delta}{120} + \frac{0.6}{T_w} + .138 b_{110} + \frac{.23}{15} \left(\frac{\partial c_p}{\partial T}\right)_w \frac{h_{t1} b_{110}^2}{c_{p_w}^2} \quad (6-7)$$

Substituting for δ^*/Δ from equation (6-7) and for θ/Δ from equation (4-20), equation (6-3) becomes

$$\begin{aligned} &.138 b_{110} \left[1 + \frac{.111 h_{t1}}{c_{p_w}^2} \left(\frac{\partial c_p}{\partial T}\right)_w b_{110} \right] \\ &= \frac{1}{T_w} \left[\frac{2}{\Delta_0} - \frac{13}{20} \right] + \frac{1}{63} \left[4.1 + \frac{79\Delta_0}{120} + \frac{\Delta_0^2}{72} \right] \end{aligned} \quad (6-8)$$

Equation (6-4) for b_{110} can be rewritten as

$$b_{110} = \frac{h_{t1} - h_w}{h_{t1}} \frac{\frac{137}{420} + \frac{\Delta_0}{144}}{\left[P_{r_w} T_w \Delta_0 \right]^{-1} + \frac{263}{2520} + \frac{5\Delta_0^2}{3024}} \quad (6-9)$$

where θ_w/Δ (equation (4-43)) evaluated at the stagnation point has been substituted for the $(\theta_w/\Delta)_0$ term in equation (6-4). It might be mentioned that the simplest form of the equation formed by eliminating b_{110} from equations (6-8) and (6-9) will be a seventh order polynomial in Δ_0 , and even then the term involving $\partial c_p/\partial T$ was considered small compared with one in order to simplify the resulting expression.

Equations (6-8) and (6-9) do not generate the final value for Δ_0 and b_{110} . The final values are obtained by an iteration process as follows. First solve equations (6-8) and (6-9) for Δ_0 and b_{110} . Using these values for Δ_0 and b_{110} calculate δ^*/Δ from equation (4-22). The temperature ratio in equation (4-22) is determined from the enthalpy distribution of equation (4-42) as a function of b_{110} and Δ_0 as determined from equations (6-8) and (6-9). This value of δ^*/Δ is

substituted into equation (6-3) which then becomes the equation from which Δ_0 is determined. With this value of Δ_0 , equation (6-9) can be used to solve for $b_{11,0}$. The iteration process can be continued until the values for $b_{11,0}$ and Δ_0 are obtained to the accuracy desired.

With Δ_0 and $b_{11,0}$ obtained such that $\frac{d\theta}{dx}$ is in the form 0/0, it is possible, by the method of L'Hospital, to evaluate the limit if one does exist. If, in equation (4-18), $F_1(x)$ is defined to be

$$F_1(x) = \left[\frac{\Delta}{\delta} + 2 \right] \frac{1}{T_w} - \frac{\theta}{\Delta} \Delta \left[2 + \frac{\delta^*}{\theta} \right], \quad (6-10)$$

then, taking the derivative of the numerator and denominator of equation (4-18) with respect to X , the following equation is obtained

$$\left[\frac{d\theta}{dx} \right]_0 = \frac{2 \mu_w T_w^3}{P_w} \left(\frac{\theta}{\Delta} \right)_0 \frac{F_1'(x)_0}{u_{s,0}'} \quad (6-11)$$

The above expression is used to determine the initial slope $\frac{d\theta}{dx}$. First, however, the terms $F_1'(x)_0$ and $u_{s,0}'$ must be evaluated. The term $F_1'(x)_0$ is defined in Appendix III, and can be reduced to a relatively simple form for a given set of conditions. The term $u_{s,0}'$ can be written

$$\left(\frac{du}{dx} \right)_0 = \frac{\sqrt{8RT_s}}{d} \quad (6-12)$$

and its derivation will be found in Appendix IV.

Also of interest at the stagnation point is the transformed boundary layer thickness Δ . This can be obtained from equation (4-15) where the term $\left(\frac{u_s}{(-\frac{dp}{dx})} \right)_0$ is obtained in Appendix IV as

$$\left[\frac{u_s}{(-\frac{dp}{dx})} \right]_0 = \frac{d}{P_{t_2}} \sqrt{\frac{RT_{t_2}}{\theta}} \quad (6-13)$$

Substituting equation (6-13) into the equation (4-15), the expression for the stagnation point boundary thickness in the transformed plane is

$$\Delta_0^2 = \frac{\mu_w \Delta_0 d T_w^2}{P_{t_2}} \sqrt{\frac{RT_{t_2}}{\theta}} \quad (6-14)$$

Once Δ_0^2 has been determined at the stagnation point, the momentum thickness θ can be obtained from equation (4-23). The heat transfer at the wall as derived in Section IV is

$$-q_{w,0} = \frac{\mu_w}{P_{r,w}} \frac{T_w}{\Delta} h_{t,0} b_{11,0} \quad (4-47)$$

and is applicable at the stagnation point when the expression for Δ_o^2 is used. Making the required substitutions

$$-\sqrt{r} q_w = \frac{h_{+1}}{Re_w} \left[\frac{P_{+2} \mu_w}{(RT_{+2})^{\frac{1}{2}}} \right]^{\frac{1}{2}} 1.178 \frac{b_{110}}{\Delta_o^{\frac{1}{2}}} \quad (6-15)$$

As a check of the stagnation-point analysis two flight conditions and two tunnel conditions were analyzed. Table I summarizes the results of the analysis. The analysis of Case I was plotted in Figure 14 along with the results of references 27, 28, and 29. The over-all agreement between the integral analysis and the above references is encouraging.

The parameter $b_{110} / \Delta_o^{\frac{1}{2}}$ appearing in equation (6-15) is basically the only unknown quantity in that equation; the other terms will be known at a given condition. The parameter $b_{110} / \Delta_o^{\frac{1}{2}}$ is plotted in Figure 15 against h_w / h_{+1} . All the points analyzed fall on one curve. This curve can be used in predicting $-\sqrt{r} q_w$ without resorting to the solutions of equations (6-8) and (6-9) to determine b_{110} and Δ_o . This curve represents a rapid method for estimating two-dimensional stagnation-point heat transfer.

VII. DISCUSSION

The analysis just presented is adequate to cover a wide range of conditions. However, there are some conditions to which it cannot be applied directly, and others to which it cannot be applied at all. The conditions at which the present analysis is limited in scope can be considered to stem from two basic problem areas:

1. Presence of strong streamwise pressure gradients.
2. Presence of vorticity in the free-stream flow.

First, consider the problem of the strong streamwise pressure gradients. In defining the velocity profile by the fourth-order polynomial in η there is a built-in limitation on Δ . For values of Δ greater than 12 the velocity profile overshoots or exhibits a velocity somewhere in the boundary layer which exceeds the free-stream value. This is physically unlikely, even under the strongest favorable pressure gradient. Yet, in analyzing high Mach number conditions there are many times when the solution to the system of equations is possible with a $\Delta > 12$, but, because of the inherent limitations on Δ , the solution to the problem must stop. Unfortunately pressure gradients strong enough to cause Δ to exceed 12 are possible in many situations, such as at the leading edge of blunt plates in hypersonic flow, and consequently occur in regions of significant interest to warrant an attempt at a solution within the framework of the basic integral analysis. Fortunately such an approach does exist. The details of this solution will be found in Appendix VI along with a summary of the pertinent equations. Only the basic features of the analysis will be discussed here.

The significant step in obtaining a solution consists in a redefinition of the basic velocity profile. Steiger (32) defines a velocity profile, which satisfies all the boundary conditions of equation (4-8), in the following manner,

$$\frac{u}{u_s} = 1 - (1-\eta)^2 \quad (7-1)$$

When this profile is used in the analysis, there are no limitations of the magnitude of α except that $\alpha \geq 2$. Since this is being proposed as an alternative solution for flow fields with strong streamwise pressure gradients, this is effectively no restriction because streamwise gradients sufficient to make $\Lambda > 12$ have values of $\alpha > 4$. The fact that the problem of strong favorable pressure gradients on cylindrical leading edges is more severe the higher the Mach number can be shown in the following manner.

The data of Figure 6, for cylindrical leading edges, illustrate the independence of the pressure distribution, when plotted as P/P_{∞} , and free-stream Mach number. This being the case, the maximum pressure gradient expressed in the form $\frac{dP/P_{\infty}}{d\phi}$, must also be independent of the free-stream Mach number and the term $\frac{dP}{d\phi}$, which is used in the analysis as $\frac{dP}{dx}$, can be obtained from

$$\frac{dP}{d\phi} = \frac{dP/P_{\infty}}{d\phi} P_{\infty} \quad (7-2)$$

Now P_{∞} increases with Mach number (for a given free-stream static pressure), consequently the maximum pressure gradient $[\frac{dP}{dx}]_{max}$ is a unique function of Mach number. Thus the problems associated with strong favorable pressure gradients will become more severe at the higher Mach numbers.

It might be noted that, contrary to the published results of reference (32), there is no unique relation between Λ and α , but there are at least three relationships which differ in all but one respect. The three equations between α and Λ can be obtained by evaluating the following expressions:

1. $\int_0^1 \frac{u}{u_s} d\eta$
2. $\left(\frac{\partial u}{\partial y}\right)_w$
3. $\left(\frac{\partial^2 u}{\partial y^2}\right)_w$

using both the polynomial profile (equation (4-10)) and the exponential profile (equation (7-1)). Assuming that there is an unique expression between α and Λ , then the above three expressions should be invariant with respect to the choice of velocity function. Evaluating the above three expressions using both velocity profiles and equating like terms yields the following three equations:

$$1. \quad \Lambda = 12 \left(\frac{3\alpha - 7}{\alpha + 1} \right) \quad (7-3)$$

$$2. \quad \Lambda = 6(a-2) . \quad (7-4)$$

$$3. \quad \Lambda = a(a-1) . \quad (7-5)$$

The one condition common to all three equations is the fact they all pass through the point $a = 4, \Lambda = 12$.

This is a very important fact when solving a numerical problem, as can be illustrated in an example. Consider an analysis which, because of the strong streamwise pressure gradient, has been started with the system of equations developed in Appendix VI. As the solution proceeds point by point around the body, the value of a will reach a peak and then decline. Anytime a becomes less than 4, the analysis can be carried on by either method. This change from one system of equations to another can be made because of the step-by-step nature of the solution. The only fact of any consequence at station X_{n+1} , is the results of the analysis at X_n , not the system of equations used to obtain the results. In the discussion of the example it has been implicitly assumed that the results obtained by either method of analysis are essentially the same in the region $2.5a \leq 4$.

The second problem area, vorticity existing in the free-stream flow, has been investigated by many authors (33, 34, 35). The basic facet of the problem is that with vorticity in the inviscid flow field the boundary condition at the outer edge of the boundary layer involving $\frac{\partial u}{\partial y}$ is no longer valid. The effects of vorticity become appreciable when the velocity gradient $\frac{\partial u}{\partial y}$ at the outer edge of the boundary layer is of the same order of magnitude as $\frac{u_s}{\delta}$ (32).

The region on the body where the inviscid velocity gradient becomes important is that point on the plate where the streamlines entering the boundary layer have passed through the highly curved portion of the shock wave. At low Reynolds numbers this occurs in the stagnation point region, but at higher Reynolds numbers this could occur on the aft portion of a long body. The vorticity problem is inherently more severe at the leading edge region. Fortunately at the leading edge of a two-dimensional blunt flat plate the vorticity interaction becomes a problem about the same time that the assumption $\delta_f \ll \delta$ breaks down. Consequently the entire analysis is invalid and there is little hope for a solution within the framework of an integral approach. The applicability of this analysis can always be checked by comparing the value of δ at the stagnation point with the leading edge radius r . If $\delta_f \approx r$, then the integral approach as formulated in this analysis will not apply.

Now the other region where vorticity can become a problem, on the aft ends of long plates, can be treated within the framework of the integral analysis in the following manner. For a constant energy flow field the vorticity at the outer edge of the boundary layer can be expressed as a function of the entropy gradient normal to the streamlines in the following manner (36),

$$\int_{\delta} = \frac{T_s}{u_s} \left(\frac{\partial s}{\partial N} \right)_{\delta} . \quad (7-6)$$

This co-ordinate N is normal to the streamlines. On the aft end of very long bodies the streamlines are very nearly parallel to the body surface and consequently gradients normal to the streamlines in that vicinity would not differ greatly from gradients normal to the body. In terms of the entropy gradient normal to the body the vorticity at the outer edge can be expressed as

$$\zeta_{\delta} = \frac{T_{\delta}}{u_{\delta}} \left(\frac{\partial S}{\partial y} \right)_{\delta} . \quad (7-7)$$

For two-dimensional flow the vorticity can also be written

$$\zeta_{\delta} = \left(\frac{\partial v}{\partial x} \right)_{\delta} - \left(\frac{\partial u}{\partial y} \right)_{\delta} \quad (7-8)$$

where the term $\left(\frac{\partial u}{\partial y} \right)_{\delta} \gg \left(\frac{\partial v}{\partial x} \right)_{\delta}$, therefore $\left(\frac{\partial u}{\partial y} \right)_{\delta}$ can be expressed as

$$\left(\frac{\partial u}{\partial y} \right)_{\delta} = - \frac{T_{\delta}}{u_{\delta}} \left(\frac{\partial S}{\partial y} \right)_{\delta} . \quad (7-9)$$

In the analysis presented in Section IV, $\left(\frac{\partial u}{\partial y} \right)_{\delta}$ was implicitly assumed to be zero and consequently the velocity gradient at the outer edge of the boundary layer was taken to be zero. With vorticity interaction, or entropy gradients, at the outer edge of the boundary layer, equation (7-9) becomes the new boundary condition on the velocity profile. The second derivative $\left(\frac{\partial^2 u}{\partial y^2} \right)_{\delta}$ will remain zero for purposes of simplifying the analysis. The experimental data of reference 9, would seem to justify this assumption.

Equation (7-9) defines $\left(\frac{\partial u}{\partial y} \right)_{\delta}$ in terms of the entropy gradient at the outer edge of the boundary layer. In order to evaluate this derivative an entropy profile of the form

$$\left(\frac{\partial u}{\partial y} \right)_{\delta} = \sum_{i=1}^3 a_i \lambda^i = \frac{S}{S_{\delta}} \quad (7-10)$$

is assumed, where λ is the co-ordinate normal to the body such that,

$$\lambda = \frac{y - \delta}{y_{\delta} - \delta} \quad (7-11)$$

The subscript δ refers to conditions at the shock wave. The boundary conditions on equation (7-10) are:

1. $\lambda = 1 \quad \frac{\partial u}{\partial y} = 1 .$
2. $\lambda = 1 \quad \frac{dS}{dy} = f(M, \theta_w) .$
3. $\lambda = 0 \quad \frac{\partial u}{\partial y} = \frac{S_{\delta}}{S_{\delta_n}} .$

24

The entropy behind the shock wave at the station in question can be found from the thermodynamic parameters of the fluid at that point. The derivative $\frac{ds}{dy}$ at $\lambda = 1$ can be determined from the shock-wave shape and the free-stream Mach number. A good representation of the shock wave downstream of the leading edge region is given by the blast-wave theory (14, 15, 16, 17, 18, 19) and there is good experimental verification of its usefulness (37, 38). The third boundary condition is connected to the basic boundary layer solution in that it is a function of the parameter R_s . The fourth boundary condition is developed from a conservation of entropy analysis. The streamline ψ_n , in addition to having a constant R_s until it enters the boundary layer, is also isentropic. Every other streamline crossing the shock wave with $\psi > \psi_n$ will cross the plane normal to the body at x_n with the same entropy it had after it crossed the shock wave. This represents a certain fixed entropy at the plane normal to the body at x_n . Equating this fixed sum $\sum S$ to the integral of the assumed profile allows the fourth coefficient to be determined from

$$\frac{\sum S}{(\rho u_s)_s} = \int_0^1 \frac{S}{S_{s_n}} d\lambda. \quad (7-13)$$

The entropy behind the shock wave, $\sum S$, and consequently the entropy of the flow in the plane normal to the body at x_n , can be determined at the shock wave from the following equation,

$$\sum S = \int_{z_{s_n}}^1 \rho(y) u(y) S(y) \frac{dz}{z_{s_n}}. \quad (7-14)$$

The terms $\rho(y)$, $u(y)$, and $S(y)$ are functions of flow conditions on the downstream side of the shock wave which can be determined once the free-stream conditions and shock-wave shape are known. The integration indicated by equation (7-14) can be carried out numerically or analytically depending on whether the ratio of specific heats is the same on both sides of the shock wave. Consequently, it is possible to determine the coefficients a_i of equation (7-10) by equating equation (7-14) to (7-13) and solving for a_i . The expression for the velocity gradient at the outer edge of the boundary layer when the vorticity is present (equation (7-9)) becomes

$$\left(\frac{\partial u}{\partial y}\right)_s = \frac{T_s S_{s_n} \frac{S}{S_{s_n}(0)} \frac{dp}{dy} - \frac{a_i T_s S_{s_n}}{(y_{s_n} - \delta) \beta_s u_s^2}}{1 - \frac{S}{S_{s_n}(0)} S_{s_n} \frac{T_s}{\beta_s u_s^2}}. \quad (7-15)$$

Equation (7-15) can then be used to define $(\frac{\partial u}{\partial y})_s$. It might be noted that to obtain a numerical value for $(\frac{\partial u}{\partial y})_s$ for any given problem conditions existing at the outer edge of the boundary layer at x_n must be known. This information would not be generally known and a straightforward solution would require adding the pertinent equations of this section to the general analysis and determining all the parameters by a simultaneous solution. This would be a lengthy procedure and as much could be obtained by solving the zero vorticity problem first and then

using the zero vorticity solution as the starting point to evaluate the effects of vorticity using the analysis just presented.

The question might next be asked: when should the vorticity correction be applied? The answer can only come from a numerical solution of a particular case. When, in the course of a solution, the streamlines entering the boundary layer are crossing the shock wave in the highly curved portion of the shock wave, it would be well to examine the term $(\partial^2 u / \partial y^2)_e$ to determine if it is of the order $\frac{u}{\delta}$. If they are of the same order, the vorticity interaction analysis should be applied to ascertain what effect, if any, the vorticity at the outer edge of the boundary layer has on boundary layer parameters.

The analysis presented in this paper is also applicable to blunt flat plates at angle-of-attack greater than zero. The only requirement is that the surface temperature and pressure distributions be available. At non-zero angle-of-attack, analytical methods for predicting pressures over the body are very unreliable and it would be expected that the pressure distribution would have to be obtained experimentally. An analysis, in basically the same form, could be developed to define the compressible boundary layer characteristics on an axi-symmetric blunt body. The essential features of such an analysis would be the same, except that for an axi-symmetric body the analysis would not be applicable at angles-of-attack other than zero because such a flow field is no longer two dimensional.

VIII. CONCLUSIONS

The Von Karman momentum integral has been extended to include prescribed wall temperature and pressure gradients. The effects of entropy gradients in the inviscid flow have been considered and a first-order correction to account for entropy gradients has been developed.

The analysis has been carried out for blunt flat plates with cylindrical leading edges at zero angle-of-attack. The analysis itself, however, is valid for any reasonable shape or angle-of-attack provided the pressure distribution and surface temperature distribution are known. The basic features could be applied to develop a similar system of equations valid for axi-symmetric bodies at zero angle-of-attack.

The problem of very high favorable pressure gradients was considered and an alternative solution developed based on a velocity profile which does not exhibit profiles in which $u > u_g$.

APPENDIX I

Derivation of the Energy Integral Equation for
Use at the Stagnation Point

If equation (4-28) is differentiated with respect to x , the following equation, can be written;

$$h_{t_1} \frac{\partial(\rho u \Theta_w)}{\partial x} = -q_w \quad (I-1)$$

Substituting for $(-q_w)$ from equation (4-47), equation (I-1) may be written

$$\frac{\partial \rho u \Theta_w}{\partial x} = \frac{\mu_w T_w}{P_{r,w} \Delta} b_w \quad (I-2)$$

Equation (I-2) can also be written

$$\rho u \frac{\partial \Theta_w}{\partial x} + \Theta_w \left(\rho \frac{\partial u}{\partial x} + u \frac{\partial \rho}{\partial x} \right) = \frac{\mu_w T_w}{P_{r,w} \Delta} b_w \quad (I-3)$$

The compressible Bernoulli equation may be expressed as

$$u du + \frac{dp}{\rho} = 0$$

and from the definition of the speed of sound it is possible to write

$$a^2 = \frac{dp}{d\rho}$$

Combining the last two equations in such a way as to eliminate $d\rho$ there results

$$\frac{d\rho}{dx} = \frac{\rho_s M_s^2}{u_s} \frac{du}{dx} \quad (I-4)$$

After substituting equation (I-4) into equation (I-3) and rearranging the terms, one obtains the following equation

$$\frac{d\Theta_w}{dx} = \frac{\mu_w T_w}{P_{r,w} \rho_s u_s} \frac{b_w}{\Delta} + \frac{\Theta_w}{\Delta} \frac{du}{dx} (M_s^2 - 1) \quad (I-5)$$

Then, if both sides of equation (I-5) are multiplied by θ_H , the following equation is obtained

$$\frac{d\theta_H^2}{dx} = 2\frac{\theta_H}{\Delta} \frac{\mu_w}{Pr_w} \frac{T_w^2}{\rho_w u_s} + \left(\frac{\theta_H}{\Delta}\right)^2 \frac{2\Delta}{u_s} \frac{\mu_w}{Pr_w} T_w^2 [M_s^2 - 1], \quad (I-6)$$

where $\left(\frac{\theta_H}{\Delta}\right)^2 \cdot \Delta^2$ has replaced θ_H^2 , with Δ^2 determined from equation (4-15) and the Bernoulli equation. Factoring $2 \frac{\mu_w T_w^2}{\rho_w u_s} \frac{\theta_H}{\Delta}$ from both terms on the right hand side of equation (I-6), one obtains the equation

$$\frac{d\theta_H^2}{dx} = \frac{2\mu_w T_w^2}{\rho_w u_s} \frac{\theta_H}{\Delta} \left\{ \frac{b_{11}}{Pr_w T_w} + \frac{\theta_H}{\Delta} \Delta (M_s^2 - 1) \right\}. \quad (I-7)$$

Equation (I-7) is used in conjunction with equation (4-18) to define the stagnation values for b_{11} and Δ .

APPENDIX II

Approximate Relationship Between $\frac{T}{T_s}$ and $\frac{h}{h_s}$

In evaluating the terms Λ and b_1 at the stagnation point the term $\frac{\delta^*}{\Delta}$ appears in the analysis in such a way that it is necessary to evaluate the integral $\int_0^1 \frac{T}{T_s} dn$. The assumed enthalpy profile implicitly defines the ratio $\frac{T}{T_s}$ but an explicit expression between $\frac{T}{T_s}$ and $\frac{h}{h_s}$ is not available, consequently an attempt is made to obtain an approximate relationship.

The expression for the relationship between $\frac{T}{T_s}$ and $\frac{h}{h_s}$ was obtained from a correlation of the data appearing in reference (26) and reference (31). The data were analyzed in the following manner. First, for assumed values of T_s equal to 360°R , 900°R , 1800°R , and 2700°R , curves of $\frac{T}{T_s}$ vs $\frac{h}{h_s}$ were drawn for pressures of $.001 \leq P/P_{s1} \leq 10$. It was observed that for each T_s there was a region of the curve which was independent of the pressure and which could be adequately represented by a straight line, of the form $\frac{T}{T_s} = A \frac{h}{h_s} + B$.

The values of the constants A and B which best fit the data of the real gas tables are $A = .92$, and $B = .08$. The curve

$$\frac{T}{T_s} = .92 \frac{h}{h_s} + .08 \quad (\text{II-1})$$

along with data from references 26 and 31 are plotted in Figure 10. As can be seen from Figure 10, the curve represented by equation (II-1) is a valid approximation for a relationship between $\frac{T}{T_s}$ and $\frac{h}{h_s}$. The expression remains valid as long as:

1. $.001 \leq \frac{P}{P_{s1}} \leq 10$
 2. $360^\circ \leq T_s \leq 2700^\circ\text{R}$
 3. $360^\circ \leq T \leq 2700^\circ\text{R}$
- (II-2)

where the surface pressure is referenced to sea level standard pressure of 2116 lb/ft².

APPENDIX III

Derivation of $\left(\frac{dF_1}{dx}\right)_0$

Let $F_1(x)_0$ be defined as

$$F_1(x)_0 = G_1(K)_0 G_2(x)_0 - K_0 (2 + G_3[K, x, b_1]_0) \quad (\text{III-1})$$

where

$$\begin{aligned} 1. \quad G_1(K) &= \frac{\theta}{\Delta} \left(\frac{\Delta}{\theta} + 2 \right) \\ 2. \quad G_2(x) &= T_n^{-1} \\ 3. \quad G_3(K, x, b_1) &= \frac{\delta^x}{\theta} \end{aligned} \quad (\text{III-2})$$

The term K is a new variable defined as,

$$K = \Lambda \left(\frac{\theta}{\Delta} \right)^2 \quad (\text{III-3})$$

or

$$4. \quad G_4(K) = \Lambda \quad (\text{III-4})$$

Using the definition of $F_1(x)_0$ (equation (III-1)), its derivative with respect to x , applicable only at the stagnation point, can be written

$$\left[\frac{dF_1}{dx} \right]_0 = \left(\frac{\partial F_1}{\partial x} \right)_0 + \left(\frac{\partial F_1}{\partial K} \right)_0 \left(\frac{dK}{dx} \right)_0 + \left(\frac{\partial F_1}{\partial b_{11}} \right)_0 \left(\frac{db_{11}}{dx} \right)_0, \quad (\text{III-5})$$

where it has been implied in equation (III-5) that:

$$\begin{aligned} 1. \quad K &= q_2(x) \\ 2. \quad b_{11} &= q_3(x) \end{aligned} \quad (\text{III-6})$$

Each term in the expression $\left[\frac{\partial F_1}{\partial x}\right]_0$ will be investigated separately.

1. $\left(\frac{\partial F_1}{\partial x}\right)_0$

$$\left(\frac{\partial F_1}{\partial x}\right)_0 = G_1 \left(\frac{\partial G_2}{\partial x}\right)_0 - K_0 \left(\frac{\partial G_3}{\partial x}\right)_0 \quad (\text{III-7})$$

Now $\frac{\partial G_2}{\partial x} = \frac{1}{T_s} \frac{dT_w}{dx}$

and $\frac{\partial G_3}{\partial x} = \left(\frac{\theta}{\Delta}\right)' \left(\frac{\partial \delta^4}{\partial x}\right)_0$. (III-8)

Also from equation (6-7)

$$\left[\frac{\delta^4}{\Delta}\right]_0 = -\left(3 + \frac{\Lambda}{120}\right) + \frac{6}{T_w} + .138 b_{11} + \frac{.23}{15} \left(\frac{\partial c_p}{\partial T}\right)_w \frac{h_{t1} b_{11}^2}{c_{p_w}^2} \quad (\text{III-9})$$

from which

$$\left[\frac{\partial \delta^4}{\partial x}\right]_0 = \frac{.6T}{T_w} \left[\frac{dT_w}{dx}\right]_0 + \frac{.23}{15} h_{t1} b_{11}^2 \left[\frac{dT_w}{dx}\right]_0 \left\{ \frac{1}{c_{p_w}^2} \left(\frac{\partial c_p}{\partial T}\right)_w - \frac{2}{c_{p_w}^3} \left(\frac{\partial c_p}{\partial T}\right)_w^2 \right\} \quad (\text{III-10})$$

Substituting equations (III-8) and (III-10) into equation (III-7) one obtains

$$\left(\frac{\partial F_1}{\partial x}\right)_0 = \left[\frac{dT_w}{dx}\right]_0 \left[\frac{\theta}{\Delta}\right]_0 \frac{1}{T_s} \left\{ 2 - \frac{.138\Lambda}{3} - \frac{.23 h_{t1} b_{11}^2 T_s}{15} \left[\frac{1}{c_{p_w}^2} \left(\frac{\partial c_p}{\partial T}\right)_w - \frac{2}{c_{p_w}^3} \left(\frac{\partial c_p}{\partial T}\right)_w^2 \right] \right\} \quad (\text{III-11})$$

The term $\left[\frac{dT_w}{dx}\right]_0$ will come from the known stagnation point wall temperature distribution.

2. $\left[\frac{\partial F_1}{\partial k}\right]_0$

$$\left[\frac{\partial F_1}{\partial k}\right]_0 = G_2 \left(\frac{\partial G_1}{\partial k}\right)_0 - [2 + G_3]_0 - K_0 \left(\frac{\partial G_3}{\partial k}\right)_0 \quad (\text{III-12})$$

where

$$\left(\frac{\partial G_1}{\partial k}\right)_0 = \left(\frac{\partial G_1}{\partial \Lambda}\right)_0 \left(\frac{\partial \Lambda}{\partial k}\right)_0 \quad (\text{III-13})$$

and

$$\left(\frac{\partial G_1}{\partial \Lambda}\right)_0 = G_1 \left[\frac{\theta^{-1}}{\Delta} \frac{\partial \theta}{\partial \Lambda} + \frac{1}{6} \left(\frac{\theta}{\Delta}\right)' \right]_0$$

(III-14)

Now

$$K = \Lambda \left[\frac{\theta}{\Delta} \right]^2$$

and

$$\left(\frac{\partial K}{\partial \Lambda}\right)_0 = \left(\frac{\theta}{\Delta}\right)_0^2 + 2\Lambda_0 \left(\frac{\theta}{\Delta}\right)_0 \left(\frac{d\theta}{d\Lambda}\right)_0$$

(III-15)

The term $\frac{1}{\theta} \frac{d\theta}{d\Lambda}$ is evaluated from equation (4-20) as,

$$\frac{1}{\left(\frac{\theta}{\Delta}\right)_0} \left[\frac{d\theta}{d\Lambda}\right]_0 = \frac{-\left[\frac{1}{3} + \frac{5\Lambda_0}{72}\right]}{37 - \frac{\Lambda_0}{3} - \frac{5\Lambda_0^2}{144}}$$

(III-16)

Substituting equations (III-14), (III-15) and (III-16) into equation (III-13) the expression for $(\partial G_1 / \partial K)_0$ becomes

$$\left(\frac{\partial G_1}{\partial K}\right)_0 = \frac{\left(\frac{\theta}{\Delta}\right)'_0}{6} \frac{33 - \frac{3}{2}\Lambda_0 - \frac{5}{48}\Lambda_0^2}{37 - \frac{\Lambda_0}{3} - \frac{25\Lambda_0^2}{144}}$$

(III-17)

The term $(\partial G_3 / \partial K)_0$ in equation (III-12) can be written

$$\left(\frac{\partial G_3}{\partial K}\right)_0 = G_3 \left(\frac{d\Lambda}{dK}\right)_0 \left[\left(\frac{\delta^{-1}}{\Delta}\right)' \frac{\partial \delta}{\partial \Lambda} - \left(\frac{\theta}{\Delta}\right)^{-1} \frac{d\theta}{d\Lambda} \right]_0$$

(III-18)

The partial derivatives of δ/Δ and θ/Δ with respect to Λ are obtained from equations (III-9) and (III-16), respectively, and $(d\Lambda/dK)_0$ comes from equation (III-15). When the proper substitutions are made, equation (III-18), for $(\partial G_3 / \partial K)_0$, can be written

$$\left(\frac{\partial G_3}{\partial K}\right)_0 = \frac{-1}{120} \left(\frac{\theta}{\Delta}\right)_0^{-3} \left[\frac{315 \frac{\theta}{\Delta} - 120 \frac{\delta}{\Delta} \left(\frac{1}{3} + \frac{5\Lambda}{72}\right)}{37 - \frac{\Lambda}{3} - \frac{25\Lambda^2}{144}} \right]_0$$

(III-19)

Substituting equations (III-17) and (III-19) back into equation (III-12) generates the following equation for $(\partial F_1 / \partial K)_0$.

$$\begin{aligned} \left(\frac{\partial F_1}{\partial K}\right)_0 &= \frac{1}{8} [21\Lambda_0 - 16] - G_3 \left[\frac{37 - \frac{2\Lambda}{3} - \frac{15\Lambda^2}{144}}{37 - \frac{\Lambda}{3} - \frac{25\Lambda^2}{144}} \right] \\ &+ \frac{G_3}{6} \left(\frac{\theta}{\Delta}\right)_0^{-1} \left[\frac{33 - \frac{3}{2}\Lambda_0 - \frac{5}{48}\Lambda_0^2}{37 - \frac{\Lambda}{3} - \frac{25\Lambda^2}{144}} \right]_0 \end{aligned}$$

(III-20)

$$3. \left(\frac{\partial F_1}{\partial b_{11}} \right)_0$$

$$\left(\frac{\partial F_1}{\partial b_{11}} \right)_0 = -K_0 \left(\frac{\partial G_2}{\partial b_{11}} \right)_0$$

where $\left(\frac{\partial G_2}{\partial b_{11}} \right)_0 = \left(\frac{\theta}{\Delta} \right)_0^{-1} \left(\frac{\partial \delta_2^*}{\partial b_{11}} \right)_0$.

The derivative $\left[\frac{\partial \delta_2^*}{\partial b_{11}} \right]_0$ can be evaluated by differentiating Equation (III-9) with respect to b_{11} and is found to be

$$\left(\frac{\partial \delta_2^*}{\partial b_{11}} \right)_0 = .138 + \frac{.46}{15} b_{11} \left(\frac{\partial C_p}{\partial T} \right)_w \frac{h_{21}}{C_p^*}$$

With the above value for the derivative $\left[\frac{\partial \delta_2^*}{\partial b_{11}} \right]_0$ the derivative $\left(\frac{\partial F_1}{\partial b_{11}} \right)_0$ becomes

$$\left(\frac{\partial F_1}{\partial b_{11}} \right)_0 = -\Delta_0 \left(\frac{\theta}{\Delta} \right)_0 \left[.138 + \frac{.46}{15} b_{11} \left(\frac{\partial C_p}{\partial T} \right)_w \frac{h_{21}}{C_p^*} \right] \quad (\text{III-21})$$

$$4. \left[\frac{dK}{dx} \right]_0$$

Starting with equation (4-23) and rearranging it such that

$$K = \frac{\theta^2}{d} \frac{\rho_w}{\mu_w} \frac{du}{dx} \frac{1}{T_w^3} \quad (\text{III-22})$$

enables the derivative $\left(\frac{dK}{dx} \right)_0$ to be obtained as

$$\left[\frac{dK}{dx} \right]_0 = K_0 \left[\frac{1}{\theta^2} \frac{d\theta^2}{dx}, \frac{d^2u}{dx^2} \left(\frac{du}{dx} \right)^{-1}, \frac{\rho_w}{\mu_w T_w^3} \frac{d \left(\frac{\rho_w T_w^3}{\mu_w} \right)}{dx} \right]_0 \quad (\text{III-23})$$

The term $\left(\frac{d\theta^2}{dx} \right)_0$ is the parameter that is being sought and the term $\frac{d^2u}{dx^2}$ is identically zero at the stagnation point.

The term $\left[\frac{d \left(\frac{\rho_w T_w^3}{\mu_w} \right)}{dx} \right]_0$ deserves a closer examination.

First

$$p_w = \frac{P_{t2}}{R T_w} \quad (\text{III-24})$$

and

$$\mu_w = \frac{\mu_s}{T_s} c T_w \quad (\text{III-25})$$

In the last expression the terms $\frac{\mu_s}{T_s} c$ are treated as constant, since $\frac{\mu_s}{T_s}$ are only convenient reference quantities. Using the above definitions for p_w and μ_w the term $p_w T_w^3 / \mu_w$ can be written

$$\frac{p_w T_w^3}{\mu_w} = \frac{P_{t2} T_w}{R \left(\frac{\mu_s}{T_s} c \right)}$$

Consequently

$$\left(\frac{\mu_w}{p_w T_w^3} \right)_0 \left(\frac{d \frac{p_w T_w^3}{\mu_w}}{dX} \right)_0 = \frac{1}{P_{t2}} \left(\frac{d P_{t2}}{dX} \right)_0 + \frac{1}{T_w} \frac{d T_w}{dX}$$

The term dP_{t2}/dX is identically zero at a stagnation point and consequently equation (III-23) reduces to

$$\left[\frac{dK}{dX} \right]_0 = K_0 \left[\frac{1}{\theta^2} \frac{d\theta^2}{dX} + \frac{1}{T_w} \frac{dT_w}{dX} \right]_0 \quad (\text{III-26})$$

5. $\left(\frac{db_{11}}{dX} \right)_0$

It has been implicitly assumed that a relationship exists such that $b_{11} = g_2(x)$. This relationship is

$$b_{11} = \frac{\frac{h_{t1} - h_w}{h_{t1}} \left[\frac{137}{420} + \frac{\Delta}{144} \right]}{\left[P_w \Delta T_w \right]^{-1} \left[\frac{263}{2520} + \frac{5\Delta}{3024} \right]} \quad (\text{6-9})$$

This expression results from setting the numerator of the energy integral equation equal to zero and substituting for the stagnation point value of θ_w/Δ . Differentiating equation (6-9) once with respect to X one obtains

$$\frac{1}{b_{11}} \left(\frac{db_{11}}{dx} \right)_0 = \frac{-C_{Pw}}{h_{t1} - h_{w1}} \left(\frac{dT_{w1}}{dx} \right)_0 + \left(\frac{d\Delta}{dx} \right)_0 \frac{1}{144} \frac{1}{\left[\frac{137}{420} + \frac{\Delta}{144} \right]}$$

$$\left[\frac{-1}{\frac{137}{420} + \frac{\Delta}{144}} \right] \frac{b_{11} h_{t1}}{h_{t1} - h_{w1}} \left\{ \left(\frac{dP_{w1}}{dx} \right)^{-1} \left(\frac{1}{T_{w1}} \frac{dT_{w1}}{dx} - \frac{1}{P_{w1}} \frac{dP_{w1}}{dx} - \frac{1}{\Delta} \frac{d\Delta}{dx} \right) + \frac{5}{3024} \frac{d\Delta}{dx} \right\}_0.$$

(III-27)

Now the term $\frac{dP_{w1}}{dx} = \frac{\partial P_e}{\partial T} \frac{dT}{dx} + \frac{\partial P_e}{\partial P} \frac{dP}{dx}$

where again the term $\frac{dP}{dx} = 0$ at the stagnation point. Hence the term $\left(\frac{dP_e}{dx} \right)_0$ can be written as

$$\left(\frac{dP_{w1}}{dx} \right)_0 = \frac{\partial P_e}{\partial T} \frac{dT_{w1}}{dx}$$

After the terms in equation (III-27) are rearranged the expression for $\left(\frac{db_{11}}{dx} \right)_0$ can finally be written as

$$\left[\frac{db_{11}}{dx} \right]_0 = \left\{ \frac{d\Delta}{dx} \left[\frac{1}{144} + \frac{h_{t1}}{h_{t1} - h_{w1}} \left(\frac{\theta_{w1}}{\Delta} \frac{1}{\Lambda} - \frac{5b_{11}}{3024} \right) \right] + \left(- \frac{dT_{w1}}{dx} \right)_0 \frac{1}{h_{t1} - h_{w1}} \left[C_{Pw} \left(\frac{137}{420} + \frac{\Delta}{144} \right) + \frac{\theta_{w1}}{\Delta} \frac{h_{t1}}{T_{w1}} \left(1 - \frac{T_{w1}}{P_{w1}} \frac{\partial P_e}{\partial T} \right) \right] \right\} \frac{b_{11}}{\frac{137}{420} + \frac{\Delta}{144}}.$$

(III-28)

Using equations (III-15) and (III-26), $\left(\frac{d\Delta}{dx} \right)_0$ can be found as

$$\left[\frac{d\Delta}{dx} \right]_0 = \left(\frac{d\Delta}{dk} \right)_0 \left(\frac{dk}{dx} \right)_0.$$

(III-29)

Combining the results from sections 1-5 of this Appendix there results an expression for $\left[\frac{d\theta^2}{dx} \right]_0$ which has the form

$$\left[\frac{d\theta^2}{dx} \right]_0 = \beta \left[- \frac{dT_{w1}}{dx} \right]$$

(III-30)

where β is some parameter dependent on b_{11} , Δ , and X .

APPENDIX IV

Derivation of $\left[\frac{du}{dx}\right]_0$

The compressible Bernoulli equation can be written

$$u_s \frac{du}{dx} = -\frac{1}{\rho_s} \frac{dp}{dx} \quad (IV-1)$$

The pressure distribution applicable to a blunt body as obtained from the modified Newtonian theory is

$$\frac{P}{P_1} = \cos^2 2X_n \left[\frac{P_{t2}}{P_1} - 1 \right] \quad (IV-2)$$

Differentiating equation (IV-2) with respect to X , the expression for the pressure gradient is obtained as

$$\frac{dP}{dx} = 2P_1 \sin 4X_n \left[\frac{P_{t2}}{P_1} - 1 \right] \quad (IV-3)$$

Combining equations (IV-1) and (IV-3), one obtains

$$\left[\frac{du}{dx}\right]_0 = \frac{2P_1 \sin 4X_n}{\rho_s u_s} \left[\frac{P_{t2}}{P_1} - 1 \right] \quad (IV-4)$$

Now at the stagnation point both $\sin 4X_n$ and u_s go to zero and the expression for $\left[\frac{du}{dx}\right]_0$ must come from L'Hospital's method for evaluating indeterminate forms. Using the method of L'Hospital, the expression for $\frac{du}{dx}$ at the stagnation point becomes

$$\left[\frac{du}{dx}\right]_0^2 = \frac{8P_1}{d^2 \rho_s} \left[\frac{P_{t2}}{P_1} - 1 \right] \quad (IV-5)$$

At the stagnation point the term $\left[\frac{P_{t2}}{P_1} - 1 \right] \approx \frac{P_{t2}}{P_1}$ which allows the velocity derivative to be written as

$$\left[\frac{du}{dx}\right]_0 = \frac{\sqrt{8RT_{t2}}}{d} \quad (IV-6)$$

The term $\left[\frac{u_s}{\frac{dp}{dx}} \right]_0$ comes up in obtaining an expression for Δ^* . It can be evaluated from equations (IV-1) and (IV-6) as follows:

$$\frac{u_{s_0}}{\left[-\frac{dP}{dx}\right]_0} = \frac{1}{\rho_s \left[\frac{dy}{dx}\right]_0}$$

$$= \frac{RT_{+2}}{P_{+2}} \frac{d}{(8RT_{+2})^{\frac{1}{2}}}$$

or

$$\frac{u_{s_0}}{\left[-\frac{dP}{dx}\right]_0} = \left[\frac{RT_{+2}}{8}\right]^{\frac{1}{2}} \frac{d}{P_{+2}}$$

(IV-7)

APPENDIX V

Method of Numerical Solution

The equations developed in Section IV can be solved in the following manner. First equations (6-8) and (6-9) are solved by trial and error to yield the stagnation point values for b_{11} and Λ . Knowledge of b_{11} and Λ enables one to calculate Δ^* and z_w from equations (6-14) and (6-15), respectively. With Λ known, it is possible to define the stagnation point non-dimensional velocity profile. This can be considered as a limiting profile, since at the stagnation point $u_s = 0$. With b_{11} known, the total enthalpy profile at the stagnation point can be defined in terms of the non-dimensional transformed co-ordinate η . Since the pressure at the stagnation point is known, the temperature profile can be obtained from real gas tables (26) and the enthalpy profile. Integrating equation (4-22) numerically, using the temperature profile obtained from the enthalpy profile, and substituting for b_{11} the value found from the solution of equations (6-8) and (6-9), the term (δ^*/Δ) can be found.

The next step is to find the stagnation point values for θ^2 and $d\theta^2/dx$. The term θ^2 is obtained from equation (4-23) with Δ^* defined in equation (6-14). The term $d\theta^2/dx$ is obtained from equation (6-11) where the terms $F_1(x)$ and u_s can be obtained, once Λ and b_{11} have been defined for a given set of conditions, from Appendix III and IV, respectively.

Once the stagnation point values for θ^2 and $d\theta^2/dx$ are known the solution can be extended to the next step. The step-by-step method of solution is necessary because the differential equation in the system (the momentum integral equation) does not have a solution in closed form. As in any numerical solution to a differential equation, the accuracy of the final solution is an important function of the step size.

The value of θ^2 at the first step is found from the stagnation point solution using the following equation,

$$\theta_n^2 = \theta_{n-1}^2 + \Delta X_n^{n-1} \left[\frac{d\theta^2}{dx} \right]_{n-1} \quad (V-1)$$

For the first step the subscript "n-1" would correspond to the stagnation point values. Consequently the necessity of the stagnation point solution is apparent. The stagnation point solution is the first link in a sequence of events that eventually leads to the solution for the boundary layer characteristics on a blunt flat plate. At the station X_n at which the analysis is being carried out the parameters $(-d\theta^2/dx)$, T_w , and P_s are known. With these parameters essentially fixed, θ^2 can be obtained by a method completely different from equation (V-1). The different method begins by arbitrarily choosing a value of z_w . This establishes a trial value for P_{*s} , the downstream total pressures, according to the shock-wave analysis of section IV. Assuming $dP/dy = 0$, the ratio P_{*s}/P_s can be computed and this, along with the total temperature, establishes the static temperature consistent with the trial z_w . The static temperature, T_s , is obtained from the following equation,

$$T_s = \left[\frac{P_s}{P_{t_s}} \right]^{\frac{\gamma}{\gamma-1}} T_{t_s}$$

(V-2)

As it is written, it is not an explicit expression for T_s because T_s is buried in the exponent $\frac{\gamma}{\gamma-1}$. But T_s can always be obtained from (V-2) by a trial and error approach. Once a trial T_s has been established, the static enthalpy and hence the velocity can be obtained. The static enthalpy is obtained from a set of real gas tables consistent with the trial T_s and the P_s which is fixed by the choice of the station to be analyzed. The trial velocity, consistent with the initial choice of x_n and arbitrary choice of z_n , is obtained from equation (4-45).

At this point the equation involving the continuity of mass, equation (4-11), is introduced into the analysis. The expression for Δ^* , equation (4-15), is substituted into equation (4-11), and the resulting equation becomes an expression for Λ as a function of the initial choice of z_n , and the trial values of T_s and u_s consistent with this choice of z_n . A trial-and-error solution of the resulting equation will yield a value for Λ consistent with the initial choice of z_n . With Λ so determined, θ^* can be determined again, this time from equation (4-23). This value of θ^* is compared with the value obtained from equation (V-1). Different values of z_n are chosen and the whole process repeated until a value of z_n is chosen such that the trial value of θ^* matches that obtained from equation (V-1). At this point the value of z_n consistent with x_n , such that the mass flow between ψ_0 and ψ_n is equal to the mass flow in the boundary layer at x_n , has been determined. Also the temperature, total pressure, ratio of specific heats and velocity at the outer edge of the boundary layer has been established.

Next the value for θ_w/Δ is determined. This is done by numerically integrating, by some approximate technique, the heat transfer between the stagnation point and x_n . Evaluation of $\int_0^{x_n} q_w dx$ allows θ_w/Δ to be evaluated from equation (4-28). With this value of θ_w/Δ equation (4-43) becomes an expression from which the parameter b_w can be obtained. With this value of b_w and the value of Λ already obtained, the heat transfer at the wall can be obtained from equation (4-47).

The term Λ is next used to define the velocity profile using equation (4-10), and both Λ and b_w are used to define the total enthalpy profile from equation (4-42). Both profiles will be in terms of the transformed co-ordinate η . To obtain the profiles in the $x-y$ plane the static temperature distribution is required.

The static temperature distribution is obtained from the total enthalpy and velocity distributions using the energy equation,

$$h = h_t - \frac{u^2}{2}$$

(V-3)

With the static enthalpy determined from equation (V-3), the static temperature can be obtained from a set of real gas tables as a function of P_s and h_s . The expression between y and η is obtained from

$$\frac{y}{\Delta} = \int_0^{\eta} \frac{T}{T_s} d\eta$$

(V-4)

Equation (V-4) can be numerically evaluated to obtain a tabular relationship between y and η . This technique will have to be repeated at each station for which plots of velocity, or temperature in the x - y plane are required. The value of y at $\eta = 1$ is by definition δ and is exactly the integral appearing in the expression for δ/Δ . Hence, at each station at least the integral $\int_0^1 \frac{T}{T_s} d\eta$ must be evaluated in order to evaluate δ/Δ from equation (4-22).

With δ/Δ evaluated, the expression for the derivative $d\theta/dx$ is now computed for the station in question from equation (4-18). The term M_s^2 in equation (4-18) is evaluated from the values of u_s , v_s , and T_s obtained in the beginning of the analysis.

At this point the boundary layer characteristics at the first station are known. The entire analysis is then repeated at the next station starting with equation (V-1) where this time the subscript $n-1$ would refer to the values of θ^n and $d\theta/dx$ just obtained. The analysis can be continued until the entire body has been analyzed.

APPENDIX VI

Derivation of the Equations for Use with Strong Favorable Streamwise Pressure Gradients

Start by defining a new velocity function such that

$$\frac{u}{u_s} = 1 - (1-\eta)^\alpha \quad [4-10]^* \quad (VI-1)$$

Equation (VI-1) satisfies all the boundary conditions of equation (4-8) and, in addition, $\delta^2 u / \delta y^2 = 0$ where $\delta \geq 3$. This is a much stronger restriction on the profile at the outer edge of the boundary layer than previously used. Evaluating the integral

$$\int_0^1 \frac{u}{u_s} \delta \eta = \int_0^1 [1 - (1-\eta)^\alpha] \delta \eta = \frac{\alpha}{\alpha+1}, \quad (VI-2)$$

which is used in equation (4-6), the equation for Z_n from the conservation of mass principle becomes

$$Z_n = \frac{\rho_s u_s}{\rho_w u_w} \frac{\Delta}{d} \frac{\alpha}{\alpha+1} \quad [4-11] \quad (VI-3)$$

Utilizing equation (VI-1) in defining Δ^2 from the momentum equation evaluated at the wall (equation (4-9)) the new expression for Δ^2 results:

$$\Delta^2 = \frac{u_s \mu_w T_w^3}{-\frac{\delta p}{\delta x}} \alpha (\alpha-1) \quad [4-15] \quad (VI-4)$$

Introducing the velocity profile into the compressible momentum equation (equation (4-16)), the following expression results:

$$\frac{\delta \theta^2}{\delta x} = - \frac{z \theta}{\Delta} \frac{T_w^3}{u_s} \frac{\mu_w}{\rho_w} \alpha \left[\frac{1}{T_w} - (\alpha-1) \left(z + \frac{\delta^2}{\theta} - M_s^2 \right) \right] \quad [4-18] \quad (VI-7)$$

At this point it might be stated that there are three relationships between Δ and α . The result is that, whenever Δ appears from $(\partial^2 u / \partial y^2)_w$, substitute $\alpha(\alpha-1)$; whenever Δ appears in the form $[\Delta + z]$ from $(\partial u / \partial y)_w$, substitute α , and whenever the term $\frac{z}{\Delta} + \frac{\delta^2}{\theta}$ appears from $\int_0^1 \frac{u}{u_s} \delta \eta$, substitute $\frac{\alpha}{\alpha+1}$. These are valid substitutions and adhering to them will convert all the equations in the main body of this report to this new velocity profile of equation (VI-1).

*Numbers in square brackets refer to the corresponding equation in main body of the analysis.

Having already evaluated $\int_0^1 \frac{4}{\bar{u}_s} d\eta$ using equation (VI-1), the expression for δ^*/Δ becomes

$$\frac{\delta^*}{\Delta} = \int_0^1 \frac{T}{T_s} d\eta - \frac{a}{a+1}. \quad [4-22] \quad (VI-8)$$

Applying the Dorodnitsyn transformation to the definition of θ/Δ (equation (4-19)) and then evaluating the integral using the new velocity profile of equation (VI-1), one obtains the following result:

$$\frac{\theta}{\Delta} = \frac{a}{(a+1)(2a+1)}. \quad [4-20] \quad (VI-9)$$

The parameter \int_2 appearing in the profile for the adiabatic wall total enthalpy distribution, can simply be converted by recognizing that $\frac{h_{+1,2}}{h_{+1}} = a$ or,

$$\int_2 = (1-P_{ew}) \frac{h_{+1} - h_s}{h_{+1} - h_{aw}} a^2. \quad [4-39] \quad (VI-10)$$

The term \int_2 does not change and is essentially zero when $\frac{\partial c_p}{\partial T} \approx 0$.

The biggest change in the whole analysis occurs in evaluating θ_w/Δ . It is a tedious but straightforward procedure and when completed the following expression for θ_w/Δ , applicable to heat transfer conditions, results:

$$\begin{aligned} \frac{\theta_w}{\Delta} = & \frac{h_{+1} - h_w}{h_{+1}} \left[\frac{3}{5} - \frac{6}{a+3} + \frac{\theta}{a+4} - \frac{3}{a+5} \right] \\ & - b_{11} \left[\frac{3}{20} - \frac{3}{a+3} + \frac{5}{a+4} - \frac{2}{a+5} \right] \\ & - [1-P_{ew}] a^2 \frac{h_{+1} - h_s}{h_{+1}} \left[\frac{1}{30} - \frac{1}{a+3} + \frac{2}{a+4} - \frac{1}{a+5} \right]. \end{aligned}$$

[4-43] (VI-11)

The recovery factor for an adiabatic wall can be obtained from equation (VI-11) by equating $b_{11} = 0$ and $\theta_w/\Delta = 0$ as was done previously. The resulting expression is

$$1-r_w = a^2 [1-P_{ew}] \left[\frac{\frac{1}{30} - \frac{1}{a+3} + \frac{2}{a+4} - \frac{1}{a+5}}{\frac{3}{5} - \frac{6}{a+3} + \frac{\theta}{a+4} - \frac{3}{a+5}} \right]$$

[5-2] (VI-12)

The stagnation-point analysis as previously presented should be adequate for all pressure gradients since $\frac{\partial p}{\partial z} = 0$ at the stagnation point. For comparison, the equations to be solved for a_0 and b_{11} will be given below,

$$b_{11} = \frac{h_{+1} - h_{aw}}{h_{+1}} \left[\frac{3}{5} \cdot \frac{6}{a_0+3} + \frac{8}{a_0+4} - \frac{3}{a_0+5} \right]$$

$$\left\{ Pr_w T_w a_0 (a_0 - 1) \right\}^{-1} + \frac{3}{20} - \frac{6}{a_0+3} + \frac{8}{a_0+4} - \frac{3}{a_0+5}$$

[6-9] (VI-13)

and

$$1.30 b_{11} \left[1 + \frac{11 h_{+1}}{c_{p_w} T_w} \left(\frac{\partial C_p}{\partial T} \right)_w b_{11} \right] = \frac{3a_0 - 8}{a_0 + 1} \left[\frac{2a_0 - 1}{2a_0 + 1} \frac{q_0}{3a_0 - 8} - \frac{1}{5T_w} \right] \quad [6-8] \quad (VI-14)$$

The equations presented above are proposed for use when the basic analysis indicates that a solution lies in the regime where $\Lambda \geq 12$. This analysis of the strong gradient case using the equations presented in this Appendix will never generate velocity profiles where $u > u_s$. It is limited to conditions where the profile parameter a is greater than 2.

APPENDIX VII

Method for Predicting Adiabatic Wall Temperatures

The adiabatic wall temperature can be determined within the framework of the Von Karman integral analysis. The following three conditions can be considered as applicable for the flow over an adiabatic wall:

1. $(b_{11})_n = 0$.
2. $\int_0^{x_n} g_w dx = 0$.
3. $\left[\frac{\theta_w}{\Delta}\right]_n = 0$.

For adiabatic flow over a plate $h_w = h_{aw}$ and, since $b_{11} = \rho_1 \frac{h_w - h_{aw}}{h_{w1}}$, it is obvious that b_{11} must be identically zero. In addition, if there is no heat transfer to the wall at any point, then the heat transfer integrated over the plate must also be zero. The condition $[\theta_w/\Delta]_n = 0$ follows directly from the second condition and equation (4-20). The requirement that there be no heat transfer to the wall eliminates the energy equation from the system of equations to be solved. In its place the expression $r_w = f(\Lambda, Re_w)$ (equation (5-2)) is used.

The adiabatic wall temperature can be defined, consistent with a prescribed pressure gradient, in the following manner.

1. Solve equation (6-3) for Λ_0 (noting $b_{11,0} = 0$).
2. Assuming that $h_{w,0} = h_{s,0}$, use equation (6-11) to determine $[\partial\theta/\partial x]_0$.
3. With Λ_0 determined from equation (6-3) and the $(\theta/\Delta)_0$ used in calculating $(\partial\theta/\partial x)_0$, evaluate θ_w^2 from equation (4-23).
4. Pick a reasonable value for $[T_{aw}]_n$ and complete the analysis of Appendix V to determine Λ and u_s consistent with the choice of $[T_{aw}]_n$.
5. Using the value of Λ , and u_s obtained in step 4, calculate $[T_{aw}]_n$ from equation (5-2).
6. Compare the value of $[T_{aw}]_n$ obtained in step 5 with the value of $[T_{aw}]_n$ assumed in step 4.

7. Repeat steps 4 and 5 at the same station until the value of $[T_{aw}]_n$ obtained in step 5 is the same value as assumed in step 4.
8. Calculate $\left[\frac{d\theta^*}{dx}\right]_n$ at the first station from equation (4-18).
9. Find θ^* at the next step from equation (V-1).
10. Start back at step 4 and repeat the analysis until T_{aw} and $d\theta^*/dx$ at this step and θ^* at the next step are known.

In the above manner the adiabatic wall temperature may be determined on any body over which the integral analysis may be applied.

BIBLIOGRAPHY

1. Chapman, D. R., and Rubesin, M. W., "Temperature and Velocity Profiles in the Compressible Laminar Boundary Layer with an Arbitrary Distribution of Surface Temperature," Jour. of the Aeronautical Sciences, Vol. 16, No. 9, pp. 547-569, September 1949.
2. Beckwith, Ivan E., "Heat Transfer and Skin Friction by an Integral Method in the Compressible Laminar Boundary Layer with a Streamwise Pressure Gradient," NACA TN 3005, September 1953.
3. Libby, Paul A., and Morduchow, Morris, "Method for Calculation of Compressible Laminar Boundary Layer with Axial Pressure Gradient and Heat Transfer," NACA TN 3157, January 1954.
4. Li, T. Y., and Nagamatsu, H. T., "Shock Wave Effects on the Laminar Skin Friction of an Insulated Flat Plate at Hypersonic Speeds," Jour. of the Aeronautical Sciences Vol. 20, No. 5, pp. 345-355, May 1953.
5. Hayes, W. D., and Probst, R. F., Hypersonic Flow Theory, Academic Press, New York, 1959.
6. Lees, L., and Kubota, T., "Inviscid Hypersonic Flow over Blunt Nosed Bodies," Jour. of the Aeronautical Sciences Vol. 24, No. 3, pp. 195-202, March 1957.
7. Wagner, Jr., Richard D., "Some Aspects of Modified Newtonian and Prandtl-Meyer-Expansion Method for Axisymmetric Blunt Bodies at Zero Angle of Attack," Jour. of the Aero/Space Sciences, Vol. 26, No. 12, pp. 851-852 December 1959.
8. Penland, Jim A., "Aerodynamic Characteristics of a Circular Cylinder at Mach Numbers 6.86 and Angles-of-Attack up to 90°," NACA TN 3861, January 1957.
9. Gregorek, G. M., Nark, T. C., and Lee, F. D., "An Experimental Investigation of the Surface Pressure and the Laminar Boundary Layer on a Blunt Flat Plate in Hypersonic Flow", ASD TDR 62-792, Volumes I and II, September 1962.
10. Martellucci, A., and Fields, A., "Pressure Distribution on Flat Plates with Surface Inclination," General Applied Science Laboratory, Inc. Technical Report No. 171, June 1960.
11. Probst, R. F., and Kemp, N. H., "Viscous Aerodynamic Characteristics in Hypersonic Rarefied Gas Flow," Jour. of the Aero/Space Sciences, Vol. 27, No. 3, pp. 174-192, March 1960.
12. Hayes, W. D., "On Hypersonic Similitude," Quarterly of Applied Mathematics, Vol. 5, No. 1, pp. 105-106, April 1947.
13. Van Dyke, M. D., "Applications of Hypersonic Small-Disturbance Theory," Jour. of the Aeronautical Sciences, Vol. 21, No. 3, pp. 179-186, March 1954.
14. Sakurai, A., "On the Propagation and Structure of the Blast Wave, I," Jour. of the Physical Society of Japan, Vol. 8, No. 5, pp. 662-669, September-October 1953.

15. Sakurai, A., "On the Propagation and Structure of the Blast Wave, II," Jour. of the Physical Society of Japan, Vol. 9, No. 2, pp. 256-266, March-April 1954.
16. Sedov, L. I., Similarity and Dimensional Methods in Mechanics, Academic Press, New York, 1959.
17. Taylor, G. I., "The Formation of a Blast Wave by a Very Intense Explosion," Proceeding of the Royal Society of London, Vol. 201, pp. 159-186, 1950.
18. Lin, S. C., "Cylindrical Shock Waves Produced by Instantaneous Energy Release," Jour. of Applied Physics Vol. 25, No. 1, pp. 54-57, January 1954.
19. Lukasiewicz, J., "Hypersonic Flow-Blast Analogy," AEDC-TR-61-4 January 1961.
20. Baum, Howard R., "Some Electron Densities in the Vicinity of a Hypersonic Blunt Body," AEDC-TN-59-101, August 1959.
21. Love, Eugene S., "A Re-examination of the use of Simple Concepts for Predicting the Shape and Location of Detached Shock Waves," NACA TN 4170, December 1957.
22. Freeman, N. C., "On the Theory of Hypersonic Flow Past Plane and Axially Symmetric Bluff Bodies," Journal of Fluid Mechanics, Vol. 1, Part 4, pp. 356-362, October 1956.
23. Moeckel, W. E., "Approximate Methods for Predicting form and Location of Detached Shock Waves Ahead of Plane or Axially Symmetric Bodies," NACA TN 1921, 1949.
24. Schlichting, H., Boundary Layer Theory, Pergamon Press, New York, 1955.
25. Ames Research Staff, "Equations, Tables and Charts for Compressible Flow," NACA TR 1135, 1953.
26. Hansen, C. F., "Approximations for the Thermodynamic and Transport Properties of High Temperature Air," NASA TR-R-50, 1959.
27. Fay, J. A., and Riddell, F. R., "Theory of Stagnation Point Heat Transfer in Dissociated Air," Jour. of the Aeronautical Sciences, Vol. 25, No. 2, pp. 73-85, February 1958.
28. Eggers, A. J., Hansen, C. F., and Cunningham, B. E., "Stagnation Point Heat Transfer to Blunt Shapes in Hypersonic Flight Including Effects of Yaw," NACA TN 4229, April 1958.
29. Hankey, W. L., Neumann, R. D., and Flynn, E. H., "Design Procedures for Computing Aerodynamic Heating at Hypersonic Speeds," WADC TR 59-610, p. 17, June 1960.
30. Feldman, S., "Hypersonic Gas Dynamic Charts for Equilibrium Air," AVCO Research Laboratory Report, January 1957.
31. Anon., "Handbook of Supersonic Aerodynamics," NAVORD Report 1488, Vol. 5, Section 15, 1950.

32. Steiger, M. H., "Integral Method Boundary Layer Calculations for Strong Favorable Streamwise Pressure Gradients," ARL TN 60-137, July 1960.
33. Ferri, Antonio, "Some Heat Transfer Problems in Hypersonic Flow," WADC TN 59-308, July 1959.
34. Ho, H. T., and Probst, R. F., "The Compressible Viscous Layer in Rarefied Viscous Flow," ARL TN 60-132, August 1960.
35. Ferri, Antonio, "A Review of Some Recent Developments in Hypersonic Flow," WADC TN 58-230, September 1950.
36. Shapiro, A. H., The Dynamics and Thermodynamics of Compressible Fluid Flow, Vol. I, Ronald Press, 1953.
37. Creager, M. O., "The Effect of Leading-Edge Sweep and Surface Inclination of the Hypersonic Flow Field Over a Blunt Flat Plate," NASA Memo 12-26-58A, January 1959.
38. Bertram, M. H., and Henderson, A., "Effects of Boundary Layer Displacement and Leading Edge Bluntness on Pressure Distribution, Skin Friction and Heat Transfer of Bodies at Hypersonic Speeds," NACA TN 4301, July 1950.

Table 1. Summary of Stagnation Point Heat Transfer Calculations

<u>CASE I</u>				
Altitude ¹ =200,000 ft		Velocity=10,000 ft/sec, r = 12 in		
h_w/h_{t1}	.429	.215	.107	.054
q_{w0}	5.77	9.07	11.54	13.40
<u>CASE II</u>				
Altitude = 250,000 ft		Velocity=15,000 ft/sec, r=12 in		
h_w/h_{t1}	.215	.107	.054	.027
q_{w0}	15.70	19.56	23.68	25.42
<u>CASE III</u>				
515 psia	2060°R	$M_1=12.28$	r = 0.5 in	
h_w/h_{t1}	.659	.821	.971	1.000
q_{w0}	1.15	.58	.07	0.00
<u>CASE IV</u>				
715 psia	1960°R	$M_1=12.84$	r = 0.375 in	
h_w/h_{t1}	.244	-	-	-
q_{w0}	10.74	-	-	-

¹Atmosphere and thermodynamic data from Reference 30.

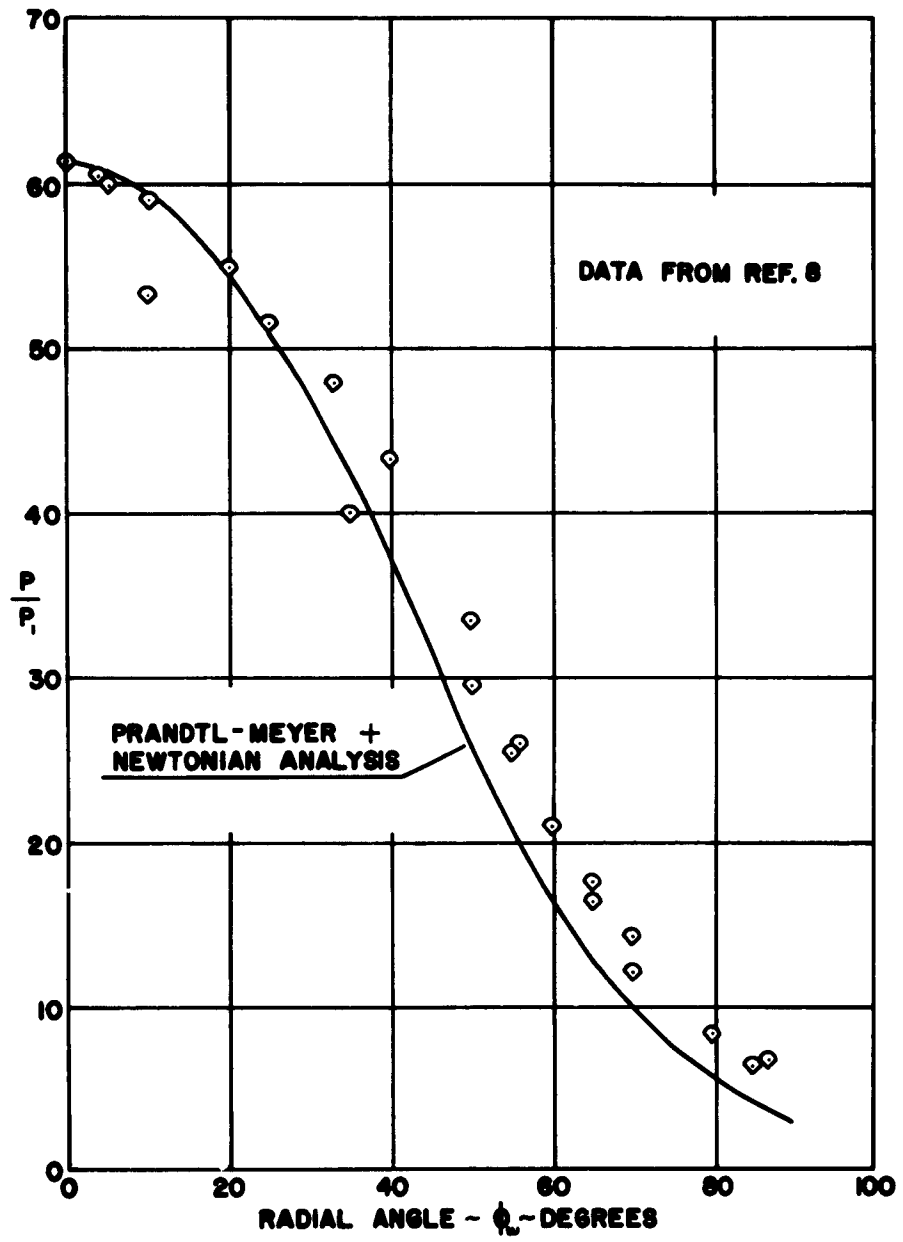


FIGURE 1. PRESSURE DISTRIBUTION OVER A CYLINDRICAL BODY AT $M_1 = 6.86$

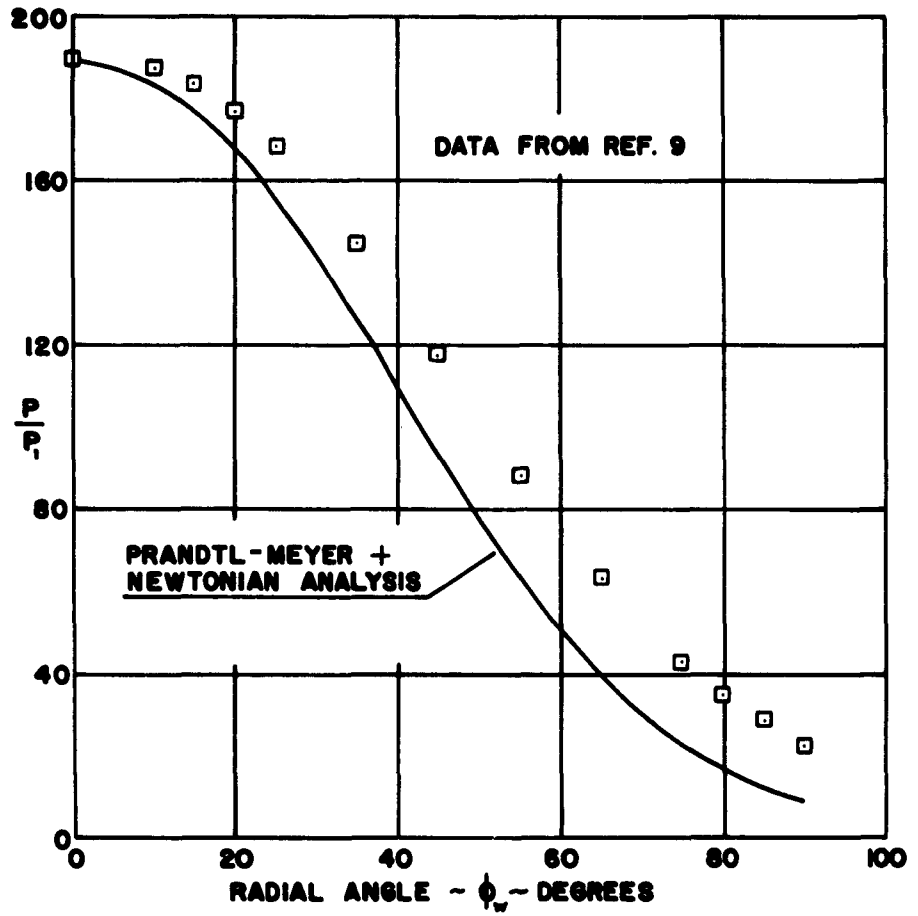


FIGURE 2. PRESSURE DISTRIBUTION OVER A CYLINDRICAL BODY AT $M_\infty = 12.26$

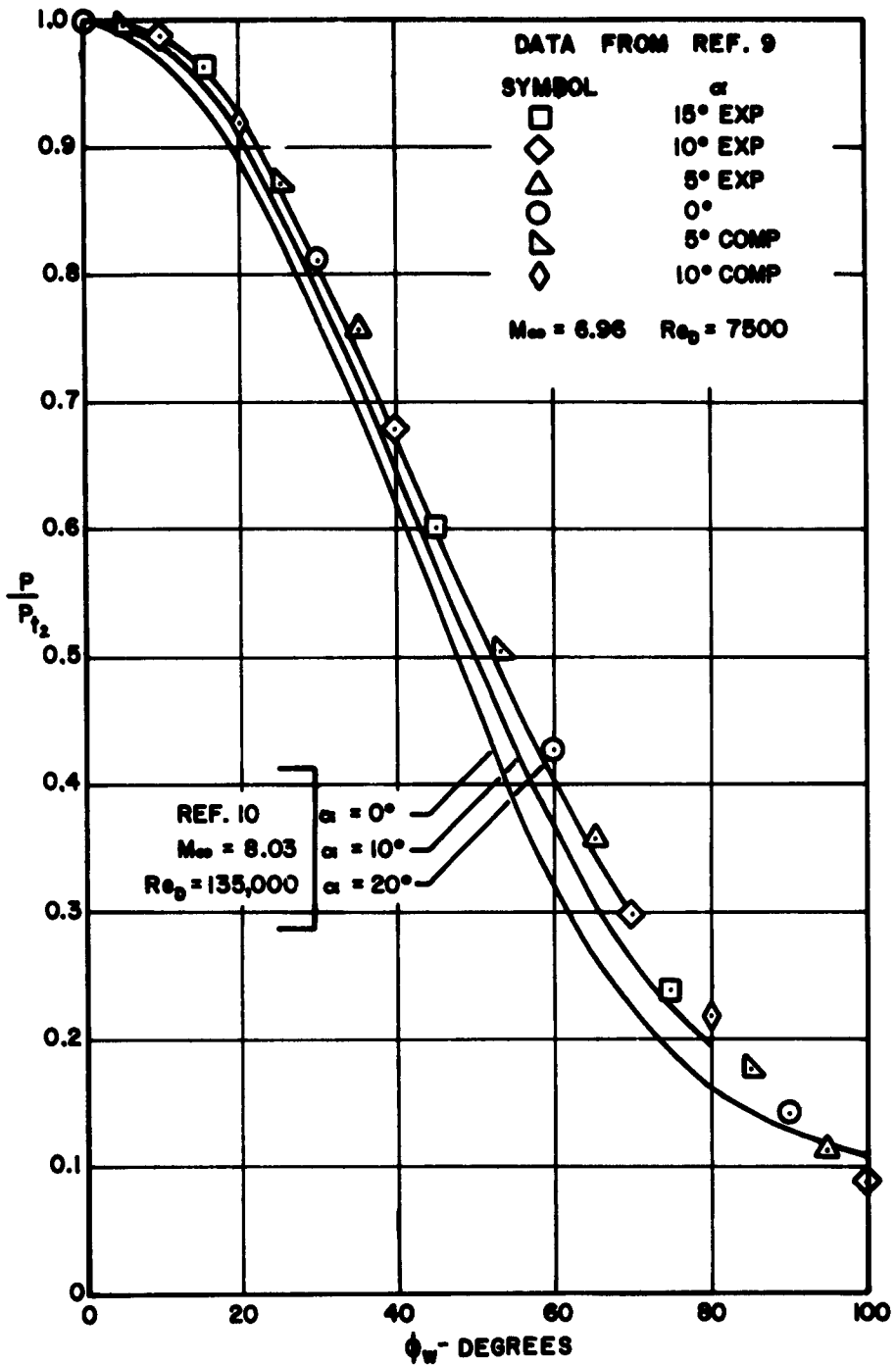


FIGURE 3. EFFECT OF ANGLE OF ATTACK ON THE PRESSURE DISTRIBUTION OVER A CYLINDRICAL LEADING EDGE

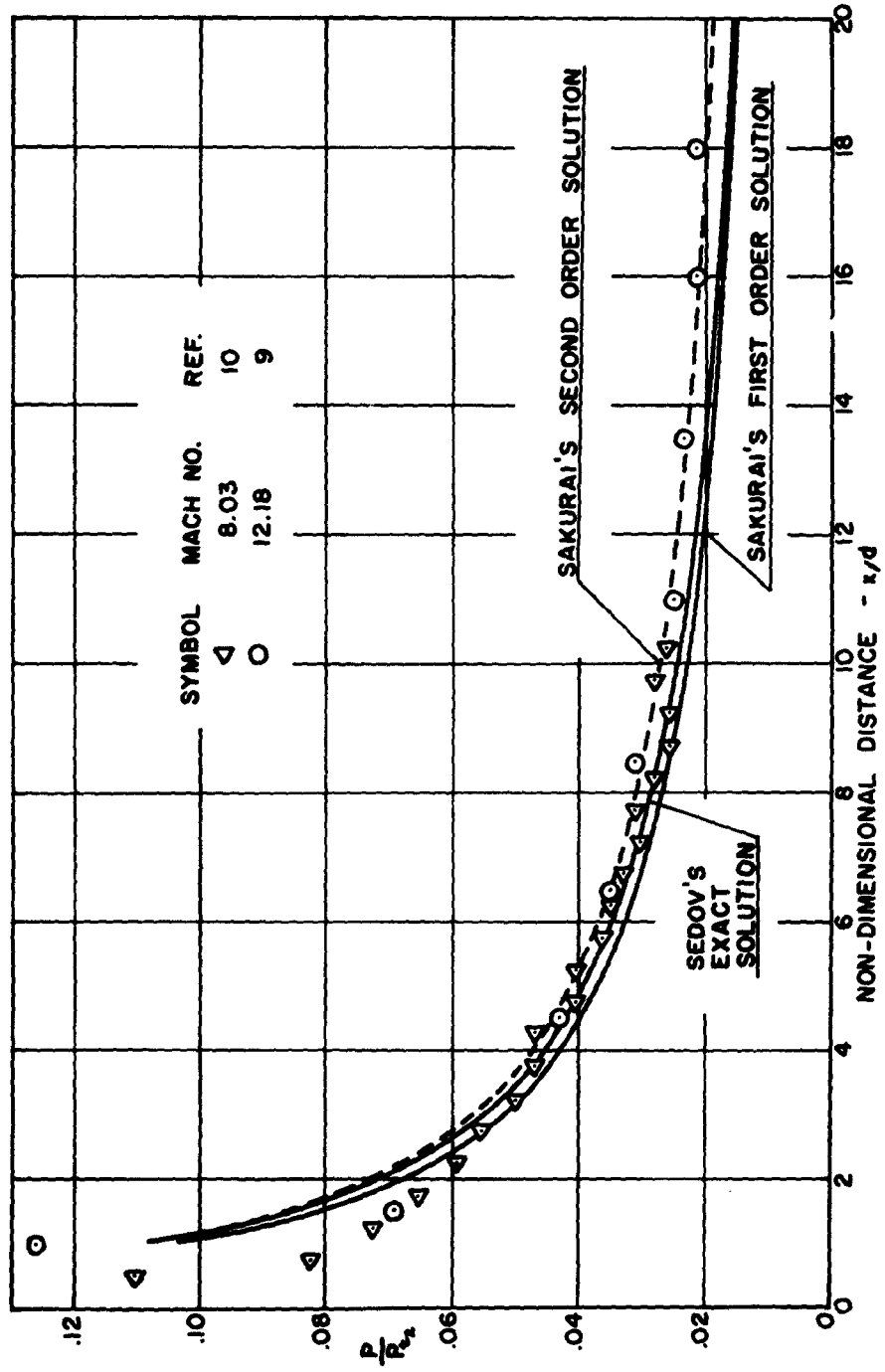


FIGURE 4. HYPERSONIC BLAST WAVE ANALOGY

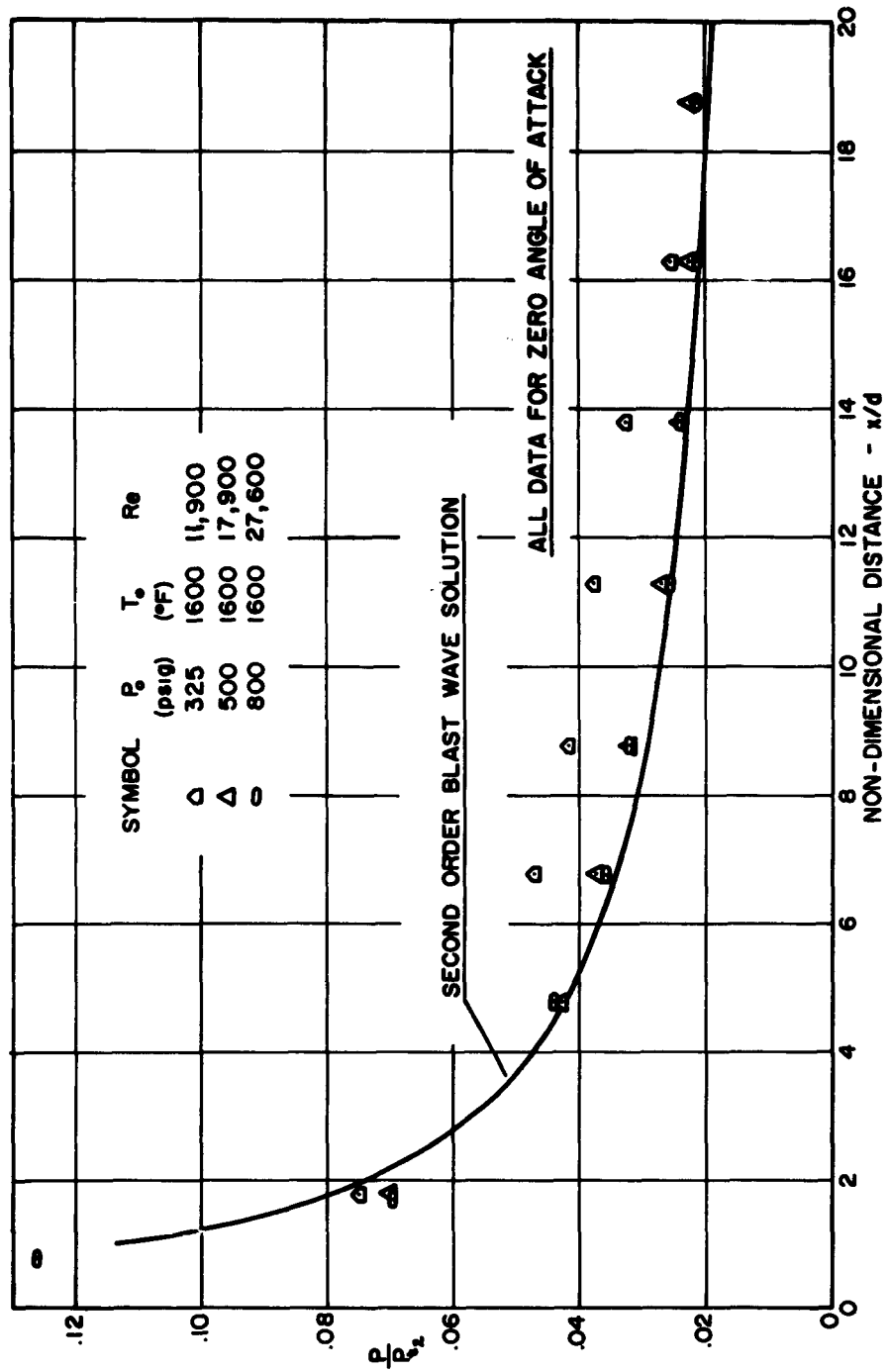


FIGURE 5. EFFECT OF REYNOLDS NUMBER ON SURFACE PRESSURE AT $M=12.2$

SYMBOL	LEADING EDGE DIA.	M ₁	REF.
□	0.5 in	12.28	9
◇	0.5 in	8.03	10
△	0.5 in	6.86	8

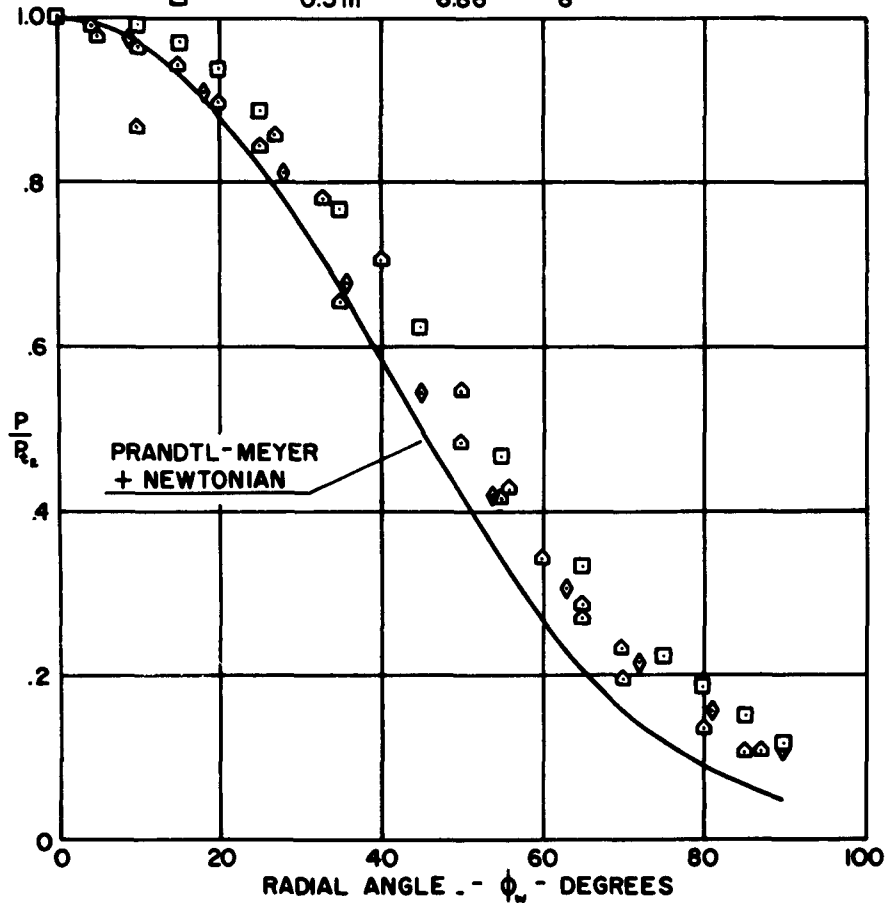


FIGURE 6. CORRELATION OF THE PRESSURE DISTRIBUTION OVER CYLINDRICAL LEADING EDGES

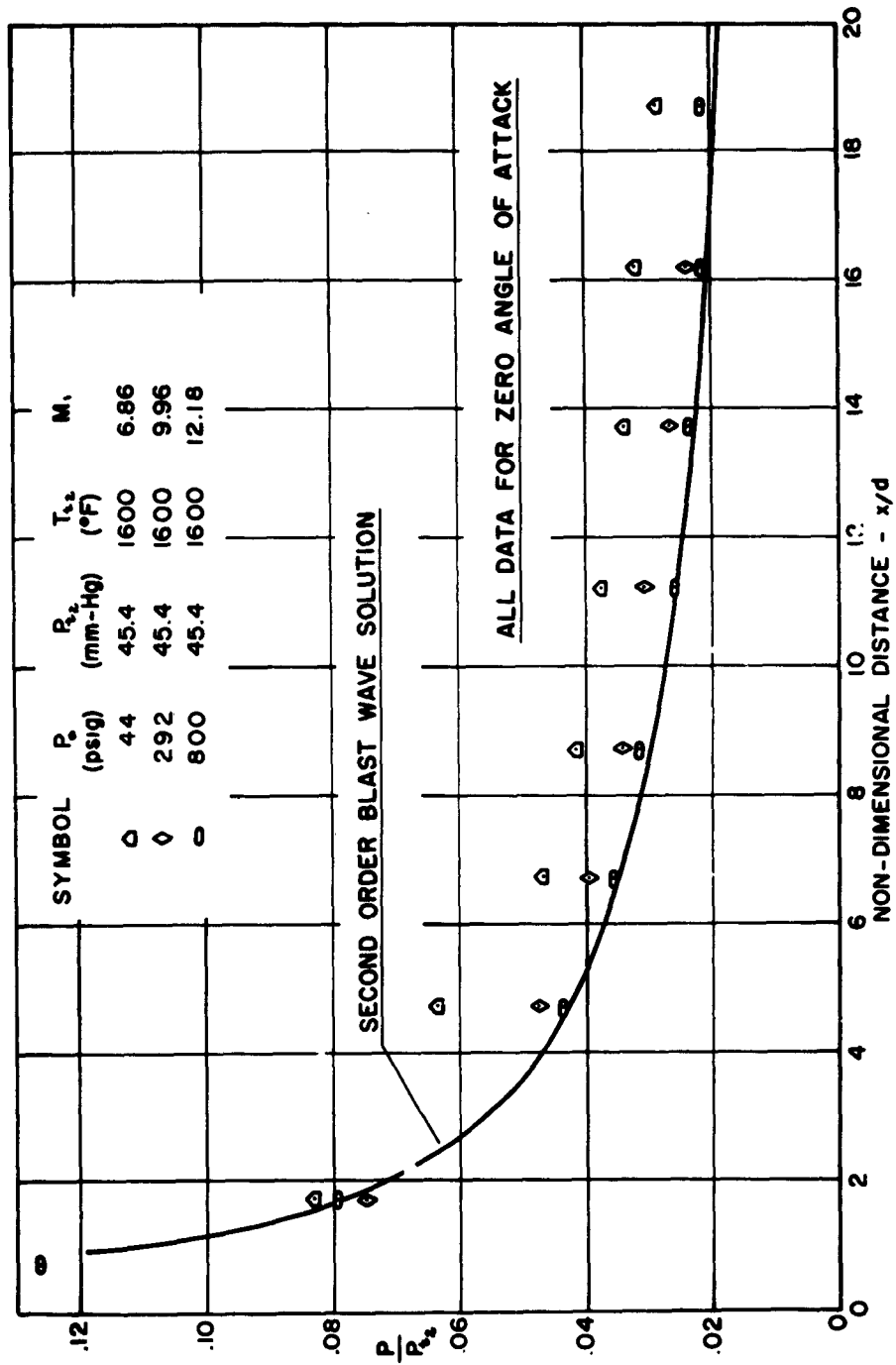


FIGURE 7. EFFECT OF M_1 ON CORRELATION OF SURFACE PRESSURES

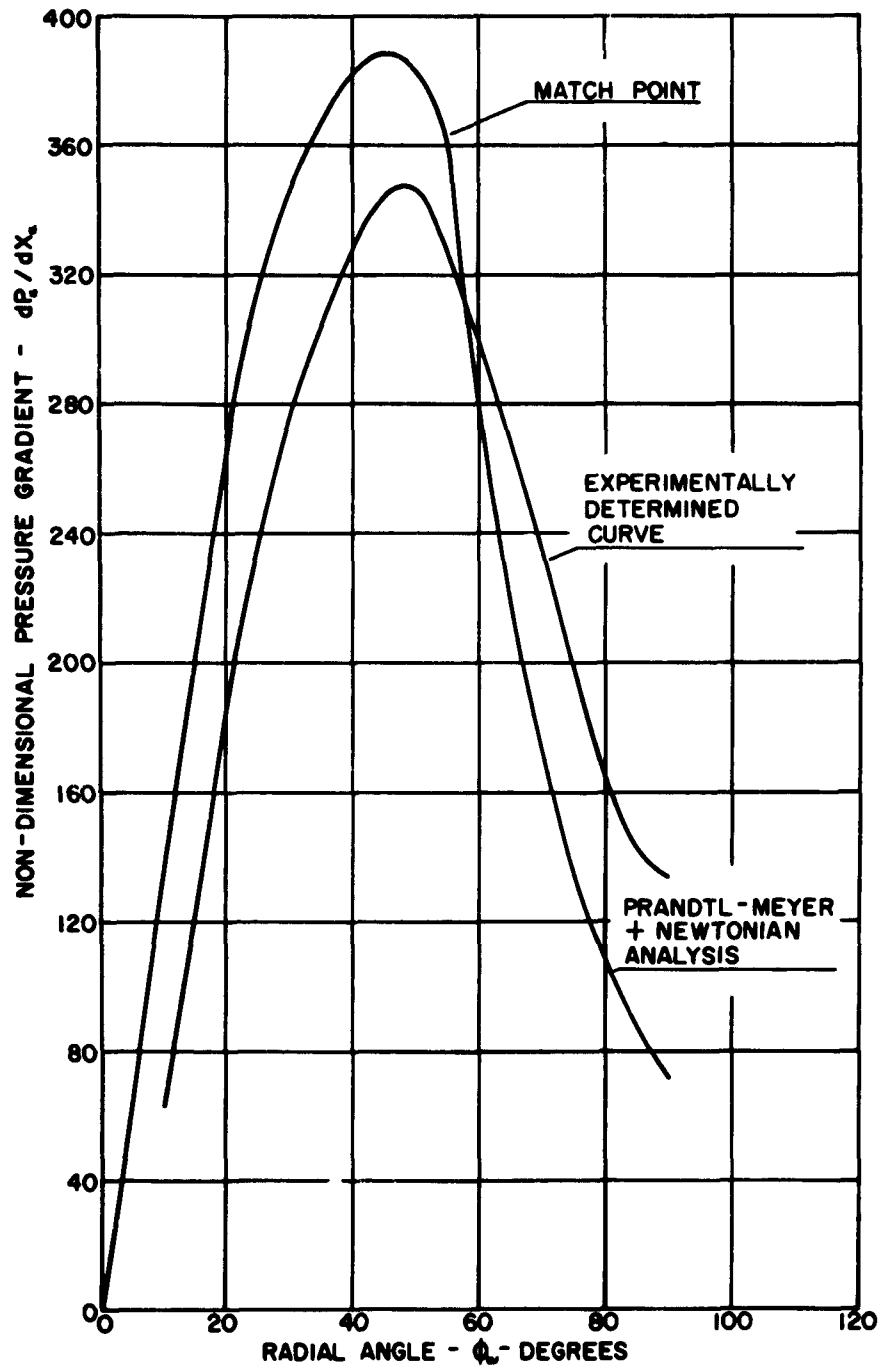


FIGURE 8. PRESSURE GRADIENT OVER A CYLINDRICAL BODY AT $M_\infty = 12.28$

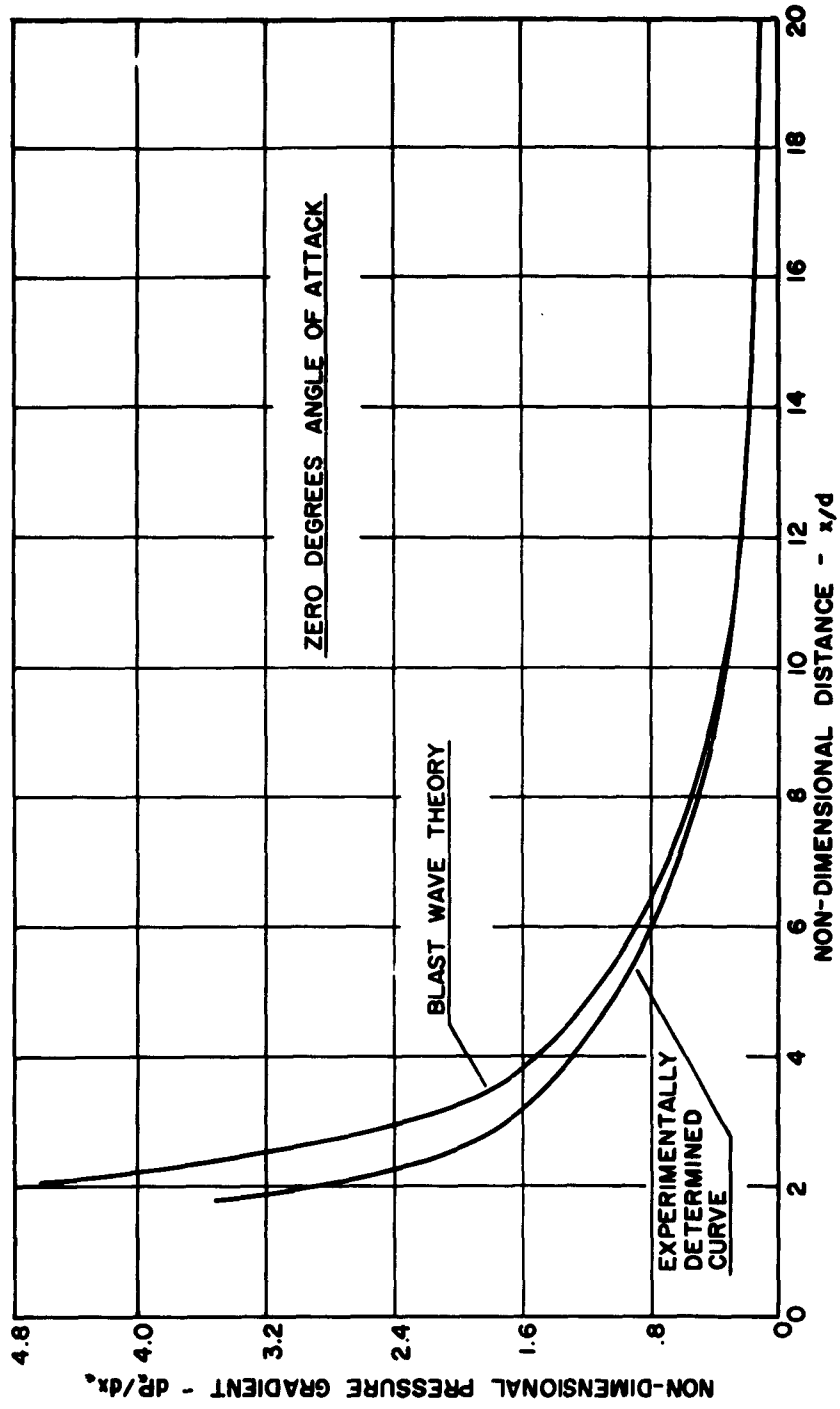


FIGURE 9. PRESSURE GRADIENT OVER A BLUNT FLAT PLATE AT $M_\infty = 12.2$

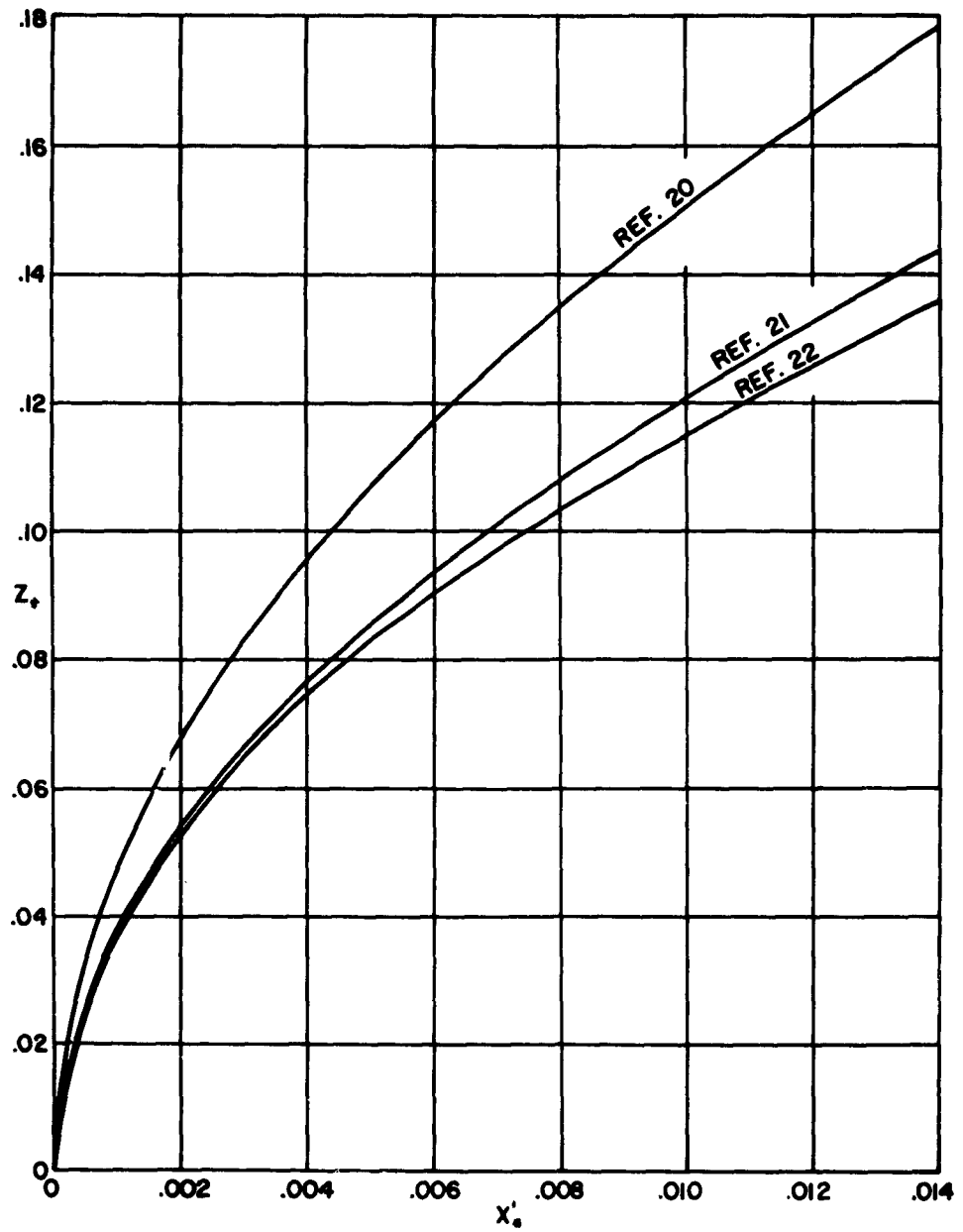


FIGURE 10. SHOCK WAVE PROFILES AT $M_\infty = 12.28$

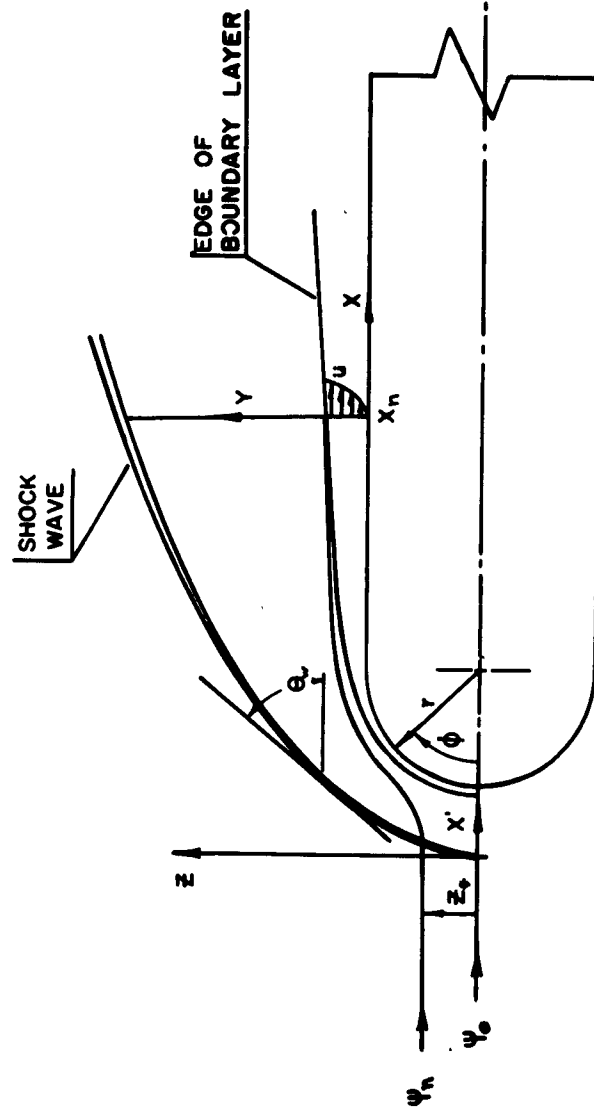


FIGURE II. COORDINATE SYSTEMS AND BODY GEOMETRY

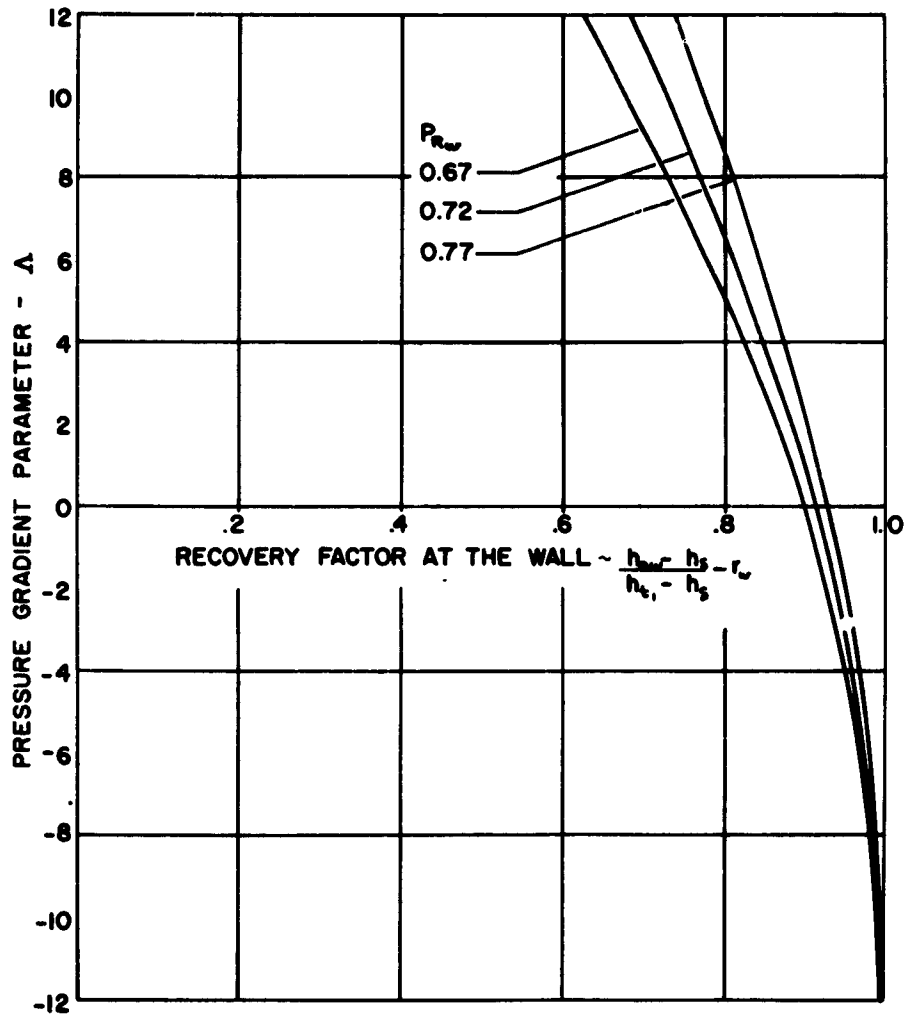


FIGURE 12. BEHAVIOUR OF THE RECOVERY FACTOR AT THE WALL WITH Pr_w

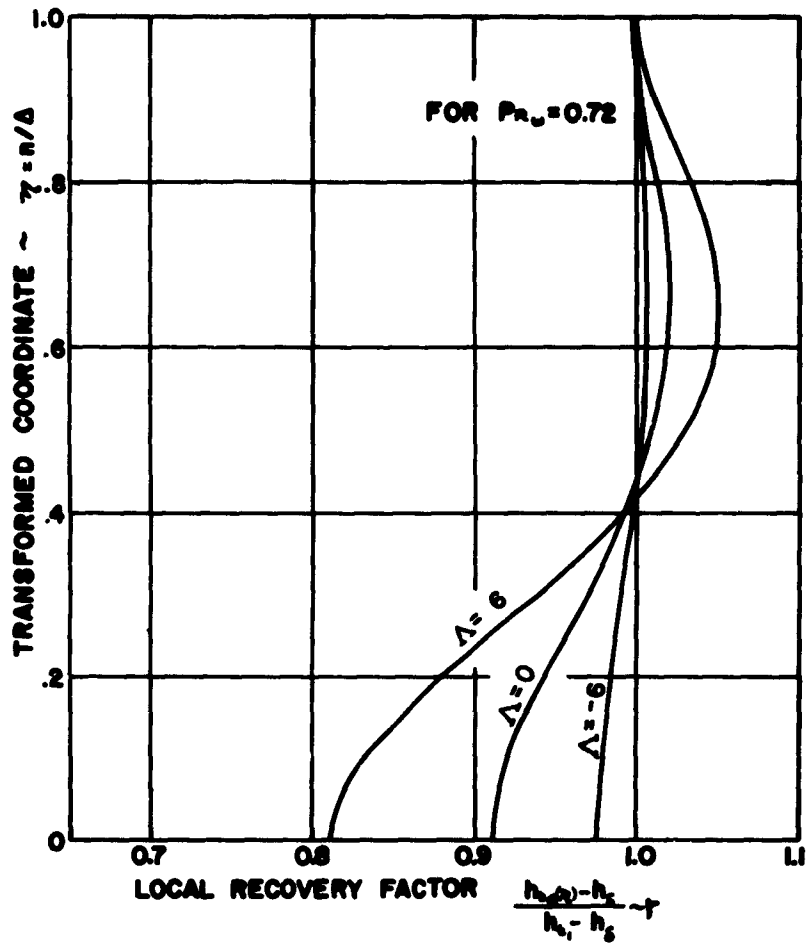


FIGURE 13. BEHAVIOUR OF THE LOCAL RECOVERY FACTOR

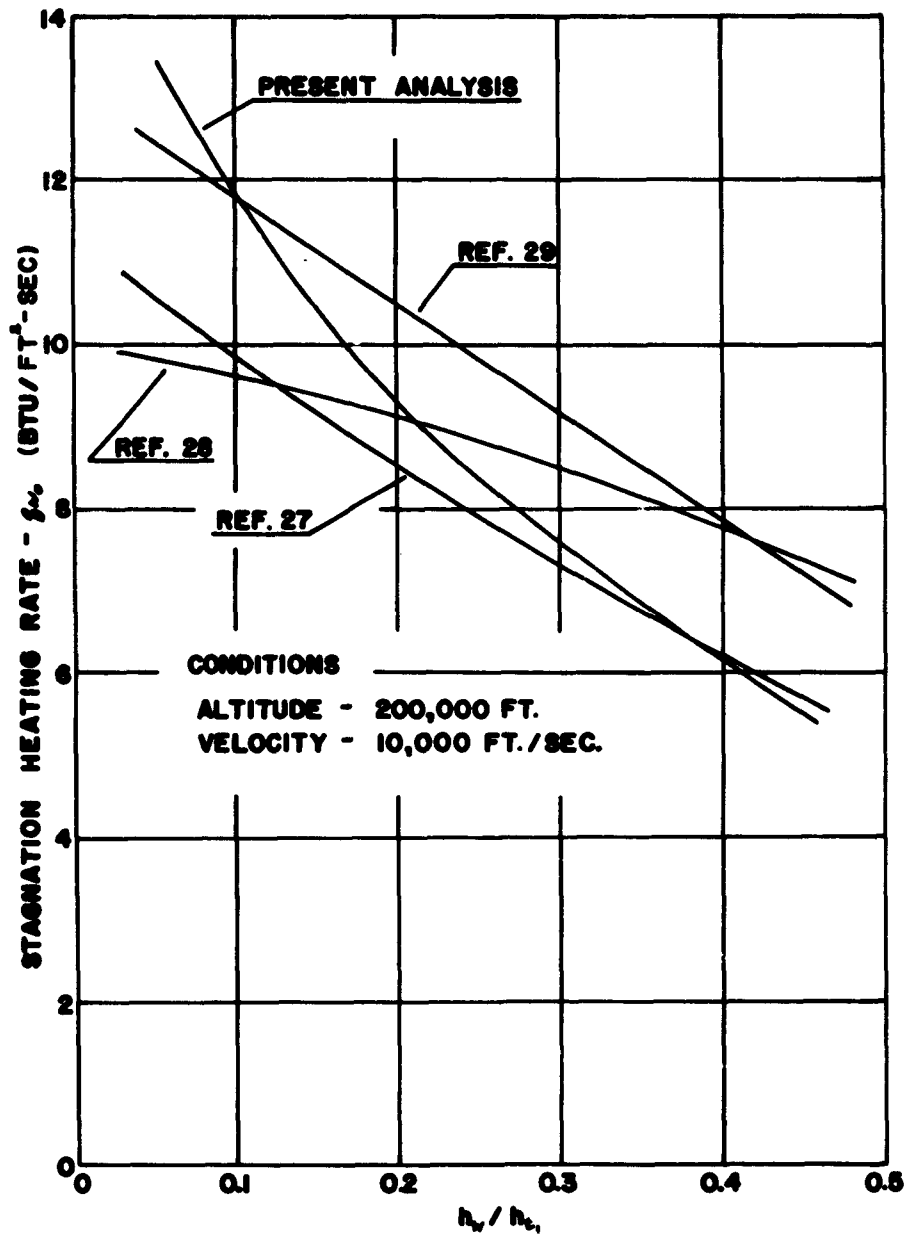


FIGURE 14. STAGNATION POINT HEAT TRANSFER COMPARISON

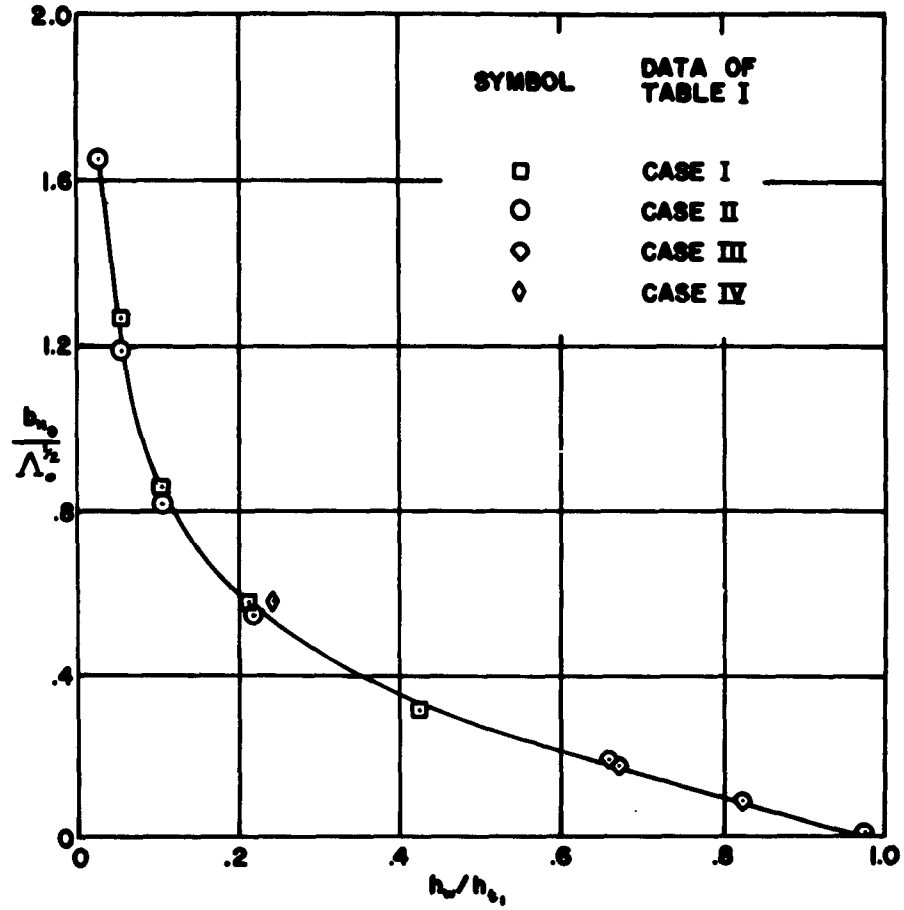


FIGURE 15. STAGNATION POINT HEAT TRANSFER CORRELATION

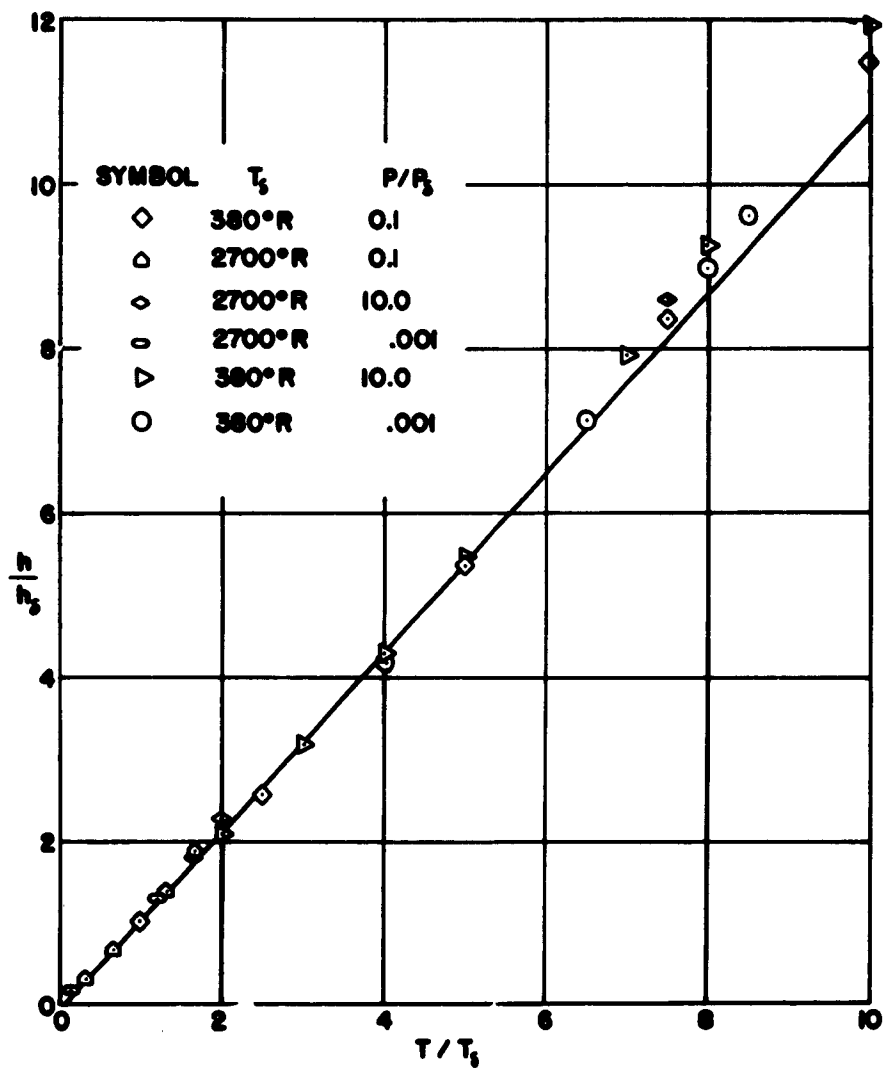


FIGURE 16. APPROXIMATION TO THE BEHAVIOUR OF A REAL GAS

1. Laminar boundary layers
2. Boundary layer
3. Compressible Flow
4. Aerodynamics
5. Hypersonic Flow
 - I. AFSC project 1366, Task 136606
 - II. Contract AF33(616)-7827

III. The Ohio State University Research Foundation, Columbus Ohio

IV. Theodore C. Mark

V. Avail fr ONS

VI. In ASTIA collection

Aeronautical Systems Division, Dir/Aero-mechanics, Flight Dynamics Lab, Wright-Patterson AFB, Ohio.

Rpt Nr ASD-TTR-62-962, THEORY OF THE COMPRESSIBLE LAMINAR BOUNDARY LAYER UNDER ARBITRARY PRESSURES AND TEMPERATURE GRADIENTS. Final report, Mar 63, 65p. Incl illus., tables, 38 refs.

Unclassified Report

An analysis is presented which can predict the compressible laminar boundary layer characteristics on a blunt flat plate with prescribed surface temperature and pressure gradients. The analysis uses a Von Karman integral method to solve the compressible

(over)

Aeronautical Systems Division, Dir/Aero-mechanics, Flight Dynamics Lab, Wright-Patterson AFB, Ohio.

Rpt Nr ASD-TTR-62-962, THEORY OF THE COMPRESSIBLE LAMINAR BOUNDARY LAYER UNDER ARBITRARY PRESSURES AND TEMPERATURE GRADIENTS. Final report, Mar 63, 65p. Incl illus., tables, 38 refs.

Unclassified Report

An analysis is presented which can predict the compressible laminar boundary layer characteristics on a blunt flat plate with prescribed surface temperature and pressure gradients. The analysis uses a Von Karman integral method to solve the compressible

(over)

1. Laminar boundary layers
2. Boundary layer
3. Compressible Flow
4. Aerodynamics
5. Hypersonic Flow
 - I. AFSC project 1366, Task 136606
 - II. Contract AF33(616)-7827

III. The Ohio State University Research Foundation, Columbus Ohio

IV. Theodore C. Mark

V. Avail fr ONS

VI. In ASTIA collection

momentum and energy equations. Problems usually encountered with very high pressure gradients are avoided by employing a new velocity profile which remains undistorted. A first-order analysis of the effect of entropy gradients in the inviscid flow on the boundary layer parameters is also given.

momentum and energy equations. Problems usually encountered with very high pressure gradients are avoided by employing a new velocity profile which remains undistorted. A first-order analysis of the effect of entropy gradients in the inviscid flow on the boundary layer parameters is also given.

